AD-A252 424

NTATION PAGE

Form Approved
OMB No. 0704-0188

1. AGENCY USE ONLY (Leave blank)	2. REPORT DATE	3. REPORT TYPE AND DATES COVERED
	24 June 1992	Technical

4. TITLE AND SUBTITLE
Interfacial Ion Transport Between Immiscible Liquids

5. FUNDING NUMBERS
C
N00014-91-J1058

6. AUTHOR(S)
Petr Vanýsek

7. PERFORMING ORGANIZATION NAME(S) AND ADDRESS(ES)
Northern Illinois University
Department of Chemistry
DeKalb, IL 60115-2862

8. PERFORMING ORGANIZATION REPORT NUMBER
Technical report
No. 042

9. SPONSORING/MONITORING AGENCY NAME(S) AND ADDRESS(ES)
Office of Naval Research
800 N. Quincy Street
Arlington, VA 2217-5000

10. SPONSORING/MONITORING AGENCY REPORT NUMBER

11. SUPPLEMENTARY NOTES
Accepted manuscript (preprint) to be published in ACS Advances in Chemistry Series No. 235.

12a. DISTRIBUTION/AVAILABILITY STATEMENT
Distribution is unlimited

12b. DISTRIBUTION CODE

13. ABSTRACT (Maximum 200 words)

The interface between two immiscible liquids is used as a characteristic boundary for study of charge equilibrium, adsorption and transport. Interfacial potential differences across the liquid/liquid boundary are explained theoretically and documented in experimental studies with fluorescent, potential sensitive dyes. The results show that presence of an inert salt or a physiological electrolyte is essential for the function of the dyes. Impedance measurements are used for studies of bovine serum albumin adsorption on the interface. Ways of determining liquid/liquid capacitance influenced by BSA presence are shown. The potential of zero charge of the interface was obtained for zero to 200 ppm of BSA. The impedance behavior is also discussed as a function of pH. A recent new approach, using microinterface for interfacial ion transport is outlined.

92-17455

92

14. SUBJECT TERMS
Ion transport, immiscible solutions, electrochemistry, fluorescent indicators, membrane potential, adsorption, impedance

15. NUMBER OF PAGES
52

16. PRICE CODE

17. SECURITY CLASSIFICATION OF REPORT	18. SECURITY CLASSIFICATION OF THIS PAGE	19. SECURITY CLASSIFICATION OF ABSTRACT	20. LIMITATION OF ABSTRACT
Unclassified	Unclassified	Unclassified	UL

OFFICE OF NAVAL RESEARCH

Contract N00014–91–J1058

Technical Report No. 042

Interfacial ion transport between immiscible liquids

by

Petr Vanýsek
Northern Illinois University
Department of Chemistry
DeKalb, IL 60115

R&T Code 413k001

Accepted manuscript (preprint) for
ACS Advances in Chemistry Series, No. 235

24 June 1992

Contribution to Membrane Electrochemistry,
Advances in Chemistry Series No. 235

edited by Martin Blank and Igor Vodyanoy

Interfacial Ion Transport between Immiscible Liquids

Petr Vanýsek

Northern Illinois University, Department of Chemistry

DeKalb, IL 60115 (U.S.A.)

{Contact: Petr Vanýsek, phone: 815–753–6876, FAX: 815–753–4802, BITNET: t40pvy1@niu}

ABSTRACT

The interface between two immiscible liquids is used as a characteristic boundary for study of charge equilibrium, adsorption and transport. Interfacial potential differences across the liquid/liquid boundary are explained theoretically and documented in experimental studies with fluorescent, potential sensitive dyes. The results show that presence of an inert salt or a physiological electrolyte is essential for the function of the dyes. Impedance measurements are used for studies of bovine serum albumin adsorption on the interface. Ways of determining liquid/liquid capacitance influenced by BSA presence are shown. The potential of zero charge of the interface was obtained for zero to 200 ppm of BSA. The impedance behavior is also discussed as a function of pH. A recent new approach, using microinterface for interfacial ion transport, is outlined.

LIQUID/LIQUID INTERFACES AND ELECTROCHEMISTRY

Interfaces between two immiscible solutions with dissolved electrolytes, most interesting to workers in several disciplines, cover theoretical physical electrochemistry, analytical applications for sensor design, and are used in interpretation of processes occurring in biological membranes and in biological systems. The interface between two immiscible electrolyte solutions was studied for the first time at least 100 years ago when Nernst (1) performed the experiments that provide the theoretical basis for today's potentiometric and voltammetric studies of interfaces. In 1963 Blank and Feig (2) suggested that an interface between two immiscible liquids could be used, at least as a crude approximation, as a model for one–half of a biological membrane. Later Koryta et al. (3) suggested, that such interface should behave similarly as an interface between an electronic conductor (i.e., an electrode) and a bathing solution. Koryta was also first to abbreviate the interface between two immiscible electrolyte solutions as ITIES. Experimental measurements revealed that this predicted similarity is real and the field of experimental electrochemistry on ITIES gained recognition and practitioners.

The similarities between ITIES and "conventional electrode" electrochemistry provide an arsenal of electrochemical techniques that have been previously tested in the more common electroanalytical chemistry and physical electrochemistry. To understand the similarities between ITIES and electrode electrochemistry, it is more useful to look at the differences first. Faradaic current flow through an electrochemical cell is associated with redox processes occurring at the electrode surface. The functional analog of an electrode surface in ITIES is the interface itself. In that case, however, the net current observed when the interface

is polarized from an outside electric source is not a result of a redox process at the interface. It is, rather, an effect that is caused by an ion transport through the interface, from one phase to another.

Figure 1 illustrates the difference in the cause of current flow experienced on an electrode and on the ITIES. Sufficiently negative potential applied to the metal electrode (A), will cause reduction of the analyte in the bathing solution. An electron will leave the electrode and reduce the dissolved species Fe^{3+} to Fe^{2+}. The overall charge balance is achieved and overall flow of negative charge from the electrode to the solution is observed. Of course, to complete the circuit an oxidation of some species, often even the solvent, has to occur on the counter electrode. Figure 1 B considers the case of ITIES with a picrate anion present in both phases. Electric potential applied between the two electrodes will result in a potential difference on the liquid interface. If the potential on the aqueous side is positive enough, the picrate anion will be carried from the nonaqueous (nitrobenzene) phase to water and its transport will appear in the outside electric circuit as a flow of negative charge from the bottom of the cell to the top. The overall charge balance is maintained by reduction of any available material of the nonaqueous phase and oxidation of some available species in the aqueous phase on surfaces of the current–carrying platinum electrodes.

LIQUID/LIQUID INTERFACES IN INTERFACIAL ION TRANSPORT

From the principle governing current/potential response of liquid/liquid electrochemistry it follows that the interface between the two immiscible electrolytes can be treated in manners similar to solid electrodes. It has to be stressed again, that it is ion transport across the interface, and not an electrode

redox process, that determines the potential and current characteristics of the system. With that in mind it is possible to employ, in some modified fashion, all the techniques used with electronic electrodes in the studies of immiscible electrolyte interfaces.

Figure 2 is a diagram of a typical cell used in the studies of immiscible electrolytes. The investigated interface is formed in the narrow part of the cell. To allow positioning of the interface within the desired location a screw–driven plunger, that varies the volume of the bottom part, can be used. In voltammetric studies, care has to be taken to eliminate voltage drop within the solutions. Since the resistance of the solvents should be eliminated, a four–electrode potentiostat with a pair of reference and counter electrodes should be used. The measured or controlled potential difference resides between the tips of the two reference electrodes, thus, the potential across the liquid–liquid (L/L) interface is monitored.

A number of techniques has been applied to the interface throughout the recent years. For the detailed list and explanations several reviews are suggested (4–11). Typical evidence of interfacial ion transport can be illustrated by Fig. 3. Here, the transport of acetylcholine cation is observed between water and nitrobenzene (curve 2). The potentials of the peaks are separated by 60 mV. This signifies a reversible process in the sense that the transported ion can move, with only thermodynamic restrictions, from one phase to another. A process that could be called irreversible is observed in the cases when the ion, upon transport to the other phase, undergoes some change that prevents its rapid return upon differential change of potential. Often this happens when the ion forms an insoluble precipitate in the opposite phase or when adsorption of the ion or its reaction product takes place on the interface. Curve 1, Fig. 3, corresponds to voltammetric curve of the

supporting electrolytes only. A reader used to study metal electrodes will observe that L/L interfaces allow much narrower potential window in which analytes can be studied. This is one disadvantage noted in electroanalytical applications of the technique.

In further work it is water/nitrobenzene interface that is described and experimentally studied. The reason for using nitrobenzene, which is not a physiologically occurring environment, is its high relative permittivity (ϵ=34.8 at 25^{o}C) that makes it very convenient for performing many studies. When the experimental techniques are perfected, in particular, when high resistance of less polar solvents can be overcome, the conclusions and experience can be expanded to the naturally occurring lipophilic environments with lower relative permittivity.

POTENTIOMETRY ON THE WATER/NITROBENZENE INTERFACE IN THE PRESENCE OF OXACYANINE DYES

The membrane or interfacial potential, particularly in biological applications, is often determined from the change in fluorescence of added oxacyanine dyes (12–13). The fluorescence intensity of the dyes depends on the solvent in which they are present. When the dyes are used as potential sensitive probes, their fluorescent intensity is a function of the interfacial potential across the membrane. Here, we studied the behavior of the transport of the dyes on a phase boundary between water and nitrobenzene to better understand the principles of the potential dye partitioning as a function of interfacial potential (14).

Oxacyanine dyes are salts, whose cations are fluorescent. To use this fluorescent property to indicate biological membrane potential, the dye cation is

added as a potentiometric indicator to a suspension of cells. If the inside of the cell has a negative potential with respect to the solution surrounding the cell, some of the dye cations will be transported across the cell membrane. The fluorescent intensity of the dye that moves from the extracellular liquid into the cell through its membrane decreases due to fluorescence quenching in a different dielectric medium or due to adsorption of the dye onto the membrane or other cell structure. This decrease in fluorescent intensity is proportional to the membrane potential and provides a relatively non–invasive and simple method of determining the cell membrane potential. A suitable technique that can be used for calibrating these probes independently *in vitro* and for understanding their behavior can be found in liquid–liquid electrochemistry research.

Interfacial potential. The relationship describing ionic equilibrium on the ITIES that accounts for all the present ions was first described by Hung (15). The derivation is based on the equality of the electrochemical potentials in either phase for all ions involved and the requirement of electroneutrality in each solvent. The equation is given as a summation over all present ions, i:

$$\sum_{i=1}^{j} z_i m_i / \{V_\alpha + V_\beta \frac{\gamma_i^\alpha}{\gamma_i^\beta} \exp[\frac{z_i F}{RT} (\Delta_\beta^\alpha \varphi - \Delta_\beta^\alpha \varphi_i^\circ)]\} = 0 , \qquad (1)$$

where z_i is the charge of the ion, m_i is the total number of moles of the ion i in both phases, V_α and V_β are the volumes of phases α (aqueous) and β (nitrobenzene), γ_i^α and γ_i^β are the activity coefficients of the ion, $\Delta_\beta^\alpha \varphi$ is the potential difference on the interface defined as $\Delta\varphi = \varphi^\alpha - \varphi^\beta$, and $\Delta_\beta^\alpha \varphi_i^\circ$ is the standard potential of transfer of the individual ion from phase α to phase β. T is absolute temperature expressed in kelvins, R is the molar gas constant (8.31441 J mol^{-1} K^{-1}) and F is the Faraday constant (96 484.6 C mol^{-1}).

The standard potential of transfer for an individual ion $\Delta_\beta^\alpha \varphi_i^\circ$ is not

amenable to thermodynamic measurement. Its value can be determined by measuring the distribution ratio of its salt for which the Gibbs free energy of transfer of the counter ion is already known. First, from the experimentally accessible partition coefficient of the salt the standard Gibbs free energy of transfer of the salt, $\Delta G^{o,\alpha\rightarrow\beta}_{tr,salt}$, from phase α to phase β is calculated as:

$$\Delta G^{o,\alpha\rightarrow\beta}_{tr,salt} = -RT \ln \frac{a_{salt}(\alpha)}{a_{salt}(\beta)} \quad . \tag{2}$$

The standard Gibbs free energy of transport of a salt is the sum of the $\Delta G^{o,\alpha\rightarrow\beta}_{tr,i}$ of both ions, so

$$\Delta G^{o,\alpha\rightarrow\beta}_{tr,i} = \Delta G^{o,\alpha\rightarrow\beta}_{tr,salt} - \Delta G^{o,\alpha\rightarrow\beta}_{tr,counterion} \quad . \tag{3}$$

Equation 3 allows to calculate the values for individual ions from the knowledge of the Gibbs energies of transfer for other individual ions. This chain calculation requires an *a priori* knowledge of the value for one ion, which is, in a rigorous thermodynamic sense, impossible. It is usually assumed that tetraphenylarsonium ($TPAs^+$) and tetraphenylborate (TPB^-) partition in the same ratio in any pair of solvents (16). Then it holds that

$$\Delta G_{tr,TPAs^+} = \Delta G_{tr,TPB^-} = (1/2)\, \Delta G_{tr,TPAsTPB} \quad . \tag{4}$$

The latter quantity is experimentally accessible from a partition ratio for the salt itself and it was used to calculate individual Gibbs energies of transfer for many ions (17). Table 1 lists the values used in this work. A corresponding standard potential of transfer for an individual ion is calculated from the standard Gibbs free energy for the transfer of individual ion from phase α to the phase β as:

$$\Delta^{\alpha}_{\beta}\varphi^{o}_{i} = \Delta G^{o,\alpha\rightarrow\beta}_{tr,i} / z_i F \quad . \tag{5}$$

Equation 1 provides a comprehensive description of the equilibrium on liquid/liquid interfaces, but it cannot be solved explicitly for $\Delta^{\alpha}_{\beta}\varphi$ without some assumption when more than two ions are involved. For more than two ions the

implicit form can be solved numerically. We used a TK–Plus Solver (Universal Technical Systems, Rockford, IL) software for a personal computer.

Reference Interface

Any system that measures potential of the liquid/liquid interface has to have a pair of reference electrodes connected to it. The aqueous phase is usually connected to a simple electrode of the second kind. The state of the nonaqueous phase is usually explored by so called reference interface, which is, in essence, an ion selective electrode. It is a liquid/liquid boundary that shares a common ion (usually a cation, denoted here B_1) of a constant and usually known concentration. The interfacial potential can be calculated as

$$\Delta_{\beta}^{\alpha}\varphi = \Delta_{\beta}^{\alpha}\varphi^{\circ}_{B_1^+} + \frac{RT}{F}\ln\left[\frac{c^{\beta}}{c^{\alpha}}\right], \tag{6}$$

under the assumption that

$$\left[\frac{c^{\beta}}{c^{\alpha}}\right]^2 \exp\left(\frac{2F}{RT}\Delta_{\beta}^{\alpha}\varphi^{\circ}_{B_1^+}\right) >> 4\left[1+\frac{c^{\beta}}{c^{\alpha}}\right]\exp\left\{\frac{F}{RT}\left(\Delta_{\beta}^{\alpha}\varphi^{\circ}_{B_1^+} + \Delta_{\beta}^{\alpha}\varphi^{\circ}_{A^-}\right)\right\}. \tag{7}$$

The counterions of the supporting electrolytes are A_1^- in phase α and A_2^- in phase β. Condition 7 has to be fulfilled for either counterion, thus designated A^-. One must realize that after bringing the two phases in contact, some repartitioning of the salts occurs. The concentrations c^{α} and c^{β} are the salt concentrations after the repartitioning, values that cannot be easily obtained. However, for the purpose of the inequality test 7 the initial concentration values before repartitioning can be used. Statement 6 is often used in the literature, but the prerequisite and the meaning of the assumption 7, first made by Hung (15), is never fully quantified. The repartitioning does not interfere with the test condition. It causes, however, significant deviation in calculated interfacial potentials in situations when inequality 7 is not fulfilled. Our calculations reveal that for reference system

consisting of tetrabutylammonium chloride (TBACl) in water and tetrabutylammonium tetraphenylborate (TBATPB) in nitrobenzene at 0.01 mol l^{-1} initial (formal) concentrations, the left hand side of eq. 7 is actually only 2.4 times greater than the right hand side. As a result, the interfacial potential for equal concentrations in both phases, calculated from eq. 6 is -248 mV, whereas the actual value obtained from eq. 1 is -245.7 mV. This difference, considering the experimental uncertainty, is acceptable. It needs to be emphasized, that any new reference system should be tested for validity of the condition 7. For example, when tetraphenylarsonium ($TPAs^+$) is the common ion in a water/nitrobenzene reference interface, the approximately calculated value is -372 mV, a significant difference from the exact value -335.5 mV (18).

Interfacial potential of the reference interface. The value of the potential of the reference interface is determined by the relative concentrations of the common ion, B_1^+, in the two phases. Thus, this interface responds to changes at the working interface through the change in the concentration of B_1^+ in the organic phase. The practical merit of the reference interface is not only that its potential can be calculated, but also its indifference to outside perturbations. For example, an attempt to change the -245.7 mV equilibrium potential of a 0.01 mol l^{-1} TBA^+/TBA^+ reference interface by 10 mV would require repartitioning of 20.5 % of all ions present in the system, a rather significant impediment to the potential change (19–20).

Other ions in the system. Consideration has to be given to what happens to the potential of the reference interface if another ion is added to the nonaqueous phase. This experimental condition will arise from ion redistribution on the working interface. Iterative calculations were made to account for the effect of the dye presence in the nonaqueous phase on the reference interface. The result shows

that if the dye concentration changes from 10^{-2} to 10^{-6} mol l^{-1} while the supporting electrolyte concentrations are held constant at 0.01 mol l^{-1}, the interface experiences only a 1 mV change. This change is so small that for actual work the potential of this interface can be considered constant.

The tetrabutylammonium chloride/tetrabutylammonium tetraphenylborate junction of equal concentrations in aqueous and oil phase are commonly used as the practical reference for L/L measurements. Often the interfacial potentials are expressed in relative terms as the potential vs. TBA^+ ion selective electrode. Potentials thus expressed are 245.7 mV lower that if they were expressed relative to the tetraphenylarsonium tetraphenylborate convention which de facto determines the practical standard scale for ITIES studies.

Nonpolarizable interface

It is important to realize, that in the case when only one salt of the type B_1A_1 is present, as in the cell 8, at respective concentrations c^{α} and c^{β} in phases α and β,

$$\begin{array}{c|c} \text{(phase } \alpha\text{)} & \text{(phase } \beta\text{)} \\ c^{\alpha} \quad B_1A_1 & B_1A_1 \quad c^{\beta} \end{array} \tag{8}$$

the interfacial potential will be independent of the total concentration of the salt. Equation 1 can be solved explicitly for one salt in the shown cell. If the charge on the cation is +n and the charge on the anion is –m then the interfacial potential can be calculated from the standard potentials of transfer of the individual ions $\Delta_{\beta}^{\alpha}\varphi$

$$\Delta_{\beta}^{\alpha}\varphi = \frac{m(\Delta_{\beta}^{\alpha}\varphi^{\circ}_{B_1^{n+}}) + n(\Delta_{\beta}^{\alpha}\varphi^{\circ}_{A_1^{m-}})}{m + n} . \tag{9}$$

If both the cation and the anion are univalent, eq. 9 simplifies to

$$\Delta_{\beta}^{\alpha}\varphi = \frac{1}{2}\,(\Delta_{\beta}^{\alpha}\varphi_{A^-}^{\circ} + \Delta_{\beta}^{\alpha}\varphi_{B^+}^{\circ}). \tag{10}$$

This system behaves as a nonpolarizable interface. The salt concentration ratio will not be affected by potential applied from an extraneous source. The equilibrium potential depends only on the standard potentials of transfer of the ions and in particular, it does not depend on the initial concentrations (c^{α} and c^{β}) nor it is a function of the phase volumes. Therefore, if only one salt is present in a L/L system, it is not amenable to potentiometric studies. It is thus essential that a supporting electrolyte be present to observe a potentiometric response of a third ion. This is similar to having immobilized ions in an ion exchanger membrane. It also explains why it is essential that a supporting electrolyte or physiological concentration of salts have to be present in measurements employing fluorescent dyes.

Ideally polarizable interface with supporting electrolytes

Supporting electrolytes are important in potentiometric determinations. A L/L system with supporting electrolytes B_1A_1 and B_2A_2 can be described by the following cell:

$$\begin{array}{cc|cc} \text{(phase } \alpha\text{)} & & & \text{(phase } \beta\text{)} \\ c^{\alpha} & B_1A_1 & B_2A_2 & c^{\beta} \end{array}. \tag{11}$$

The salts chosen as supporting electrolytes must conform to certain rules. It is essential that the ions in water are very hydrophilic, which means in the terms of the potentials of transport for the ions that

$$\Delta_{\beta}^{\alpha}\varphi_{B_1^+}^{\circ} >> 0 \text{ and } \Delta_{\beta}^{\alpha}\varphi_{A_1^-}^{\circ} << 0\,. \tag{12}$$

The salt in the nonaqueous phase must be very lipophilic:

$$\Delta_{\beta}^{\alpha}\varphi_{B_2^+}^{\circ} << 0 \text{ and } \Delta_{\beta}^{\alpha}\varphi_{A_2^-}^{\circ} >> 0\,. \tag{13}$$

Only very little repartitioning of the supporting electrolyte salts is expected for such a system. These are the conditions which are true for the supporting electrolytes, such as LiCl in water and TBATPB in nitrobenzene. Under the described conditions eq. 1 can be solved explicitly for the interfacial potential giving the following result:

$$\Delta_\beta^\alpha\varphi=\frac{RT}{2F}\ln\left\{\frac{c^\alpha\exp\left[\frac{z_i F}{RT}(-\Delta_\beta^\alpha\varphi^\circ_{A_1^-})\right]+c^\beta\exp\left[-\frac{z_i F}{RT}(-\Delta_\beta^\alpha\varphi^\circ_{B_2^+})\right]}{c^\alpha\exp\left[-\frac{z_i F}{RT}(\Delta_\beta^\alpha\varphi^\circ_{B_1^+})\right]+c^\beta\exp\left[\frac{z_i F}{RT}(\Delta_\beta^\alpha\varphi^\circ_{A_2^-})\right]}\right\}. \quad (14)$$

Potential of the supporting electrolyte. The actual equilibrium potential expressed by this equation is of little importance. It can be shown that any imposition of extraneous potential will happen without much opposition because the change requires only minute ionic repartitioning. The case can be illustrated by response of the interface consisting of 0.01 mol l^{-1} LiCl in water and 0.01 mol l^{-1} TBATPB in nitrobenzene.

Repartitioning. When the two phases are brought in contact, repartitioning equal to 0.0017 % of all ions present has to take place to establish equilibrium. The equilibrium potential will be 58.2 mV. Upon applying a 100 mV step on the interface from an outside source, only 0.035 % of total ions will have to repartition to achieve the new equilibrium. This contrasts markedly with the reference interface, where only a 10 mV potential step requires a 20.5 % concentration change.

The minimal repartitioning upon applying a potential difference on this interface is reflected by only negligible current flow. This behavior is observed within the limits of the standard potentials of transfer of the ions present in the potential window region of the system (c.f., Fig. 3). For the above TBATPB/LiCl system, the potential window is limited on the positive end by TPB^-

($\Delta^{a}_{\beta}\varphi^{\circ} = 372$ mV) and on the negative end by TBA^{+} ($\Delta^{a}_{\beta}\varphi^{\circ} = -248$ mV).

The potential described by eq. 14 will become also unimportant if an analyte ion capable of repartitioning is added to the system. Within the described potential window it is possible to observe voltammetric response due to the presence of ions whose potentials of transport are between those of the supporting electrolytes. Any ion that can partition within the potential window will take the function of the potential poising species. Therefore a supporting electrolyte, which is necessary for potentiometry of partitioning ions, does not interfere with the measurement.

Experimental procedure for potentiometry

The two dyes described here, 3,3'–diethyloxadicarbocyanine iodide and 3,3'–dimethyloxacarbocyanine iodide ($DiOC_2(5)$ and $DiOC_1(3)$), were obtained from Molecular Probes, Inc., (Eugene, OR). Their fluorescent behavior was described earlier (21–22). These two dyes were chosen for our experiment because their potentials of transfer fall within the potential window of the used supporting electrolytes. The apparatus used for the potential measurements is similar to that shown in Fig. 2, with only the reference electrodes used. The cell composition is shown in diagram 15.

$$\begin{array}{ccccccc} \text{Ag/AgCl} & \left|\begin{array}{c}\text{TBACl}\\ \text{aqueous}\end{array}\right. & \left|\begin{array}{c}\text{TBATPB}\\ \text{nitro–}\\ \text{benzene}\end{array}\right. & \left|\begin{array}{c}\text{LiCl}\\ \text{aqueous}\end{array}\right. & \text{Ag/AgCl} & & (15)\\ & & \text{RI} & & \text{WI} & & \end{array}$$

The supporting electrolytes, when used, were 0.01 mol l^{-1} lithium chloride in aqueous phase and 0.01 mol l^{-1} tetrabutylammonium tetraphenylborate (TBATPB) in nitrobenzene.

The interface of experimental interest is labeled on the diagram WI,

working interface. (RI) is the constant potential or reference interface (*vide supra*). Its aqueous phase is 0.01 mol l^{-1} tetrabutylammonium chloride. The interfacial potential of the reference interface is poised by the concentration ratio of tetrabutylammonium, an ion of a constant concentration shared by both phases. The exact potential of the reference interface can be calculated using eq. 1. The electrochemical cell is connected to an electric circuit via two Ag/AgCl electrodes immersed in an aqueous chloride solution.

Potentiometric results

As shown earlier, a single salt concentration variation does not have any effect on the interfacial potential. Thus, to study the effect of the dye cation on the interfacial potential, other ions must be present. As was discussed, supporting electrolytes selected in such a way that an ideally polarizable interface is formed when the dye is absent, are conveniently used.

Physiologically relevant to the experiment is the function of sodium chloride as the aqueous supporting electrolyte. Fig. 4 shows the variation of interfacial potential as a function of the dye concentration at selected concentrations of sodium chloride. The value 0.12 mol l^{-1} (7 g l^{-1} NaCl) corresponds to a physiological concentration.

Supplemental curves in Fig. 5 give an insight into the effect of the supporting electrolyte concentration. To underscore the importance of the supporting electrolytes in the function of the dye separation, the result is also given for iodide form of the dye in the absence of any supporting electrolytes (curve E). As expected, the potential established on the interface by the dye alone is constant, invariable of the dye concentration. Calculated interfacial potential *vs.* dye concentration is shown for the following organic phase supporting electrolyte

cations: tetramethylammonium (TMA^+), tetraethylammonium (TEA^+), tetrabutylammonium (TBA^+), tetraphenylarsonium ($TPAs^+$) and crystal violet (CV^+) with tetraphenylborate as the counterion. Lithium chloride is the aqueous phase supporting electrolyte.

Because numerical analysis reveals that it is the relative concentration, rather that its absolute value, which determines the interfacial potential, the results of these calculations are plotted as the interfacial potential *vs.* the logarithm of the ratio (base electrolyte)/(dye) (Fig. 6). This graph shows a linear plot over the range of concentration ratios between 1:10 and $1:10^{-5}$. For dye concentrations from 10^{-3} to 10^{-5} mol l^{-1} the supporting electrolyte concentration that allows to work in the linear region is between 0.01 to 1.0 mol l^{-1}. Concentration 0.01 mol l^{-1} was selected for this study.

Equation 1 shows that the ratio of the volumes of the two phases is related to the interfacial potential. Table II gives the slopes of the potential–concentration relationships for water to nitrobenzene volume ratios between 10^{-5} and 10^5. These slopes show that to approach the ideal linear voltammetric slope of 55 mV/decade in the dye concentration range of 10^{-3} to 10^{-5} mol l^{-1}, the water/nitrobenzene volume ratio should be between 1:1 and 33:1. The broadest range of the dye concentration having linear slope is 10^{-2} to 10^{-6} mol l^{-1}, at a volume ratio of 10:3. To simplify the calculations and experimental set up, equal volumes of water and nitrobenzene are often used. If activation coefficients in both phases are also assumed to be equal, eq. 1 becomes:

$$\sum_{i=1}^{j} z_i c_i / \{1 + \exp[-\frac{z_i F}{RT} (\Delta_\beta^\alpha \varphi - \Delta_\beta^\alpha \varphi_i^\circ)]\} = 0, \qquad (16)$$

where c_i is the sum of the concentrations of the ion i in the two phases.

The plots of calculated interfacial potential as a function of $DiOC_1(3)$

concentration are shown in Fig. 7 together with the experimental results for $DiOC_1(3)$ and $DiOC_2(5)$. In the range of dye concentration from 10^{-2} to 10^{-6} mol l^{-1} the measured values agree with those predicted through calculations.

The theoretical slope of the ideal linear potentiometric response 55 mV/decade is different from the intuitively expected 59 mV. This difference is easy to understand qualitatively. A tenfold increase in concentration in one phase will be followed by a subsequent repartitioning of all the ions present. Since repartitioning is aiding the interfacial potential by maintaining the interfacial equilibrium, less than the 59 mV change is needed. The slope of the experimental curve is 52±1 mV/decade.

Interfering ions. Experimental points in Fig. 7 show that at lower dye concentrations the potential attains a constant value while the calculation still predicts a change with the slope of 55 mV/decade. This disagreement can be explained by presence of an ionic impurity which poises the interfacial potential at low dye concentration. Figure 8 is a three dimensional plot illustrating the difference between the calculated interfacial potential with and without added interfering ion at 10^{-5} mol l^{-1}. The standard potential of transfer for the interfering or impurity salt was chosen to be −100 mV for its cation and +100 mV for its anion. Presence of this assumed species takes effect at dye concentrations below 10^{-5} mol l^{-1} at water–nitrobenzene volume ratios between 0.1 and 100. The flat region corresponds to composition in which the added salt (impurity) has no effect on the observed potential.

Further simulations, not shown here, were performed in which the impurity was assumed to be a lithium salt of an interfering anion present in aqueous solution. The impurity caused an increase in the slope of the potential-concentration relationship below 10^{-4} mol l^{-1} of the dye. Conversely, a cationic impurity

will cause the slope to decrease at dye concentrations below 10^{-5} mol l^{-1} when a chloride salt of the impurity is included in the calculations. The reason for discrepancy between experimental and calculated data in Fig. 7 must be some contamination in the system. The source of the contaminant is probably nitrobenzene itself. It cannot be its typical contaminant aniline, which is too hydrophilic. A higher, more lipophilic analog is a likely cause. It is important to realize that calculations show that protons (pH), at least at concentrations below 10^{-3} mol l^{-1}, have negligible effect on the established interfacial potential.

Concluding remarks on potentiometry

Due to the unique characteristics of the liquid/liquid interface system, additional factors other than concentration of analyte ion must be considered in potentiometric studies. These factors include the nature and concentration of the supporting electrolytes and the relative volume of the phases in contact. Numerical solutions of the theoretical relationship derived by Hung (15) are useful in predicting the effect of such factors as volume of the phases and concentration of added ions. Experimental results with an oxacyanine dye in a water–nitrobenzene system show a linear response in the 10^{-3} to 10^{-5} mol l^{-1} concentration range. This corresponds to a dynamic range of these dyes, when used as potential sensors, of about 120 mV. This agrees with measurements on biological membranes that show a linear range over 100 mV (23–25). Deviation from linear behavior at low dye concentrations appears to be caused by a cationic impurity in one of the phases. Similar limits on the linear range of dye–potential studies observed in biological systems are most likely due to the other ions present in the cellular fluid. Additional experiments using chelating agents to mask the effects of these interfering ions would be necessary to determine the effect of chelating these ions

on the interfacial potential and thus the feasibility of this approach.

Insensitivity to pH. Calculation and experiments show that pH will not affect the potential measurement if the pH is between 3 and 7. This is an important finding as any buffers in the liquid/liquid system complicate the system by increasing the number of ionic components. Acidity will, however, be important if the dissociation of the transported ion will be affected by pH. In our calculations, complete dissociation of all ions was assumed.

PROTEIN ADSORPTION ON WATER/NITROBENZENE INTERFACE

Adsorption on the L/L interface can be observed in voltammetric curves, but a more sensitive indication of adsorption can be obtained from impedance measurements. Voltammetric studies (26–27) showed that addition of proteins to a so called blocked (i.e., ideally polarizable) aqueous/nitrobenzene interface resulted in narrowing of the potential window of the supporting electrolyte system. This would imply that the difference in hydrophilic/hydrophobic properties of the two solvents decreased. This is explained by postulating a formation of a third phase between the original two, which would allow mediated, easier transport of the supporting electrolyte ions.

There were earlier studies of adsorption on L/L interfaces, that involved phospholipids (28–31). In our work we chose a protein as the adsorbing material, to investigate possibilities to study a less defined material (32). We used bovine serum albumin (BSA) with a molar mass of 69 000 (CRG–7, Armour Pharmaceutical Company). The preparation is known to contain certain amount of fatty acids. The same starting material was used throughout the measurement. The aqueous protein solutions were prepared fresh from a dry sample before each

experiment. The effects of BSA on the imaginary and real impedance and interfacial capacitance of water/nitrobenzene interface are discussed under varying BSA concentration, temperature and pH.

Impedance measurements. These experiments were carried out with the 1250 Frequency Analyzer and 1286 Four Electrode Potentiostat (Solartron). The cell, similar to that in Fig. 2, was equipped with a thermostated water jacket. In impedance studies it was desirable to keep the interfacial capacitance small. That way the time constant of the system was also small and the pertinent impedance could be studied in the frequency range of 1–100 Hz. Larger capacitances shift the frequencies below 1 Hz, which poses experimental difficulties. Therefore, an interface of only 2 mm diameter was studied.

Figure 9 shows a complex impedance plane plot of the water/nitrobenzene interface containing 0.01 mol l^{-1} LiCl in the aqueous phase and 0.01 mol l^{-1} tetrabutylammonium tetraphenylborate (TBATPB) in the nitrobenzene phase as the supporting electrolytes (filled circles). Upon addition of 3 ppm BSA (empty circles) the low frequency values change dramatically, which implies that addition of the protein to the system causes a change in the interfacial structure, especially in the capacitance of the interface.

The impedance response displays significant dependence on the applied interfacial potential (Fig. 10). It can be deduced from the data analysis (32) that the protein adsorbs at the interface. At more negative potentials the aqueous side of the interface has a negative surface charge (anions) and at more positive potentials it has a positive surface charge (cations). It is an important result that the curves of imaginary impedance vs. interfacial potential change and the curve maxima shift when BSA is added to the system. This suggest that the BSA is adsorbed at the interface, causing the distribution of the charging ions in the

interface to be altered.

Calculation of interfacial capacitance. From the data it is possible to obtain approximate value for the potential of zero charge (pzc). If a simple Randles circuit is assumed (Fig. 11), then the maximum of the curve $-Z_I$ vs. E corresponds to the pzc of the system. Figure 12 shows how the potential of zero charge changes in the presence of BSA. The gradual increase with increasing concentration from 1 to 6 ppm is due to the gradual formation of a monolayer of BSA on the interface. The decrease at higher concentrations is explained by formation of a thick layer having character of a third interface. Figure 13 displays the curves of a real and imaginary impedance as a function of BSA concentration at constant interfacial potential, 0.35 V (vs. TBA^+ ion selective reference interface). Important is the dramatic change in the imaginary (out of phase) impedance as a function of the protein concentration.

Imaginary component of the impedance gives a qualitative picture of the changing interfacial capacitance, but to obtain the capacitance value, the value has to be interpreted from a correctly devised equivalent circuit. Here we used the simple Randles circuit (Fig. 11). The procedure we used here was similar to that used by Wandlowski et al. (30–31). The total impedance Z of the Randles circuit is:

$$Z = R_S + 1/((1/jX_C) + 1/((Z_W/\sqrt{2}) - j(Z_W/\sqrt{2}))) . \qquad (17)$$

$X_C = -1/\omega C$ is the interfacial reactance, R_S is the bulk (solution) resistance, C is the capacitance of the interface, Z_W is the Warburg impedance, ω is the circular frequency of the applied perturbing signal and j is the imaginary unit. After separating the real and imaginary components, one obtains the following relationship for calculating the interfacial reactance:

$$X_C = (Z_I^2 + (Z_R - R_S)^2)/(Z_I + Z_R - R_S) . \qquad (18)$$

The real and imaginary impedances Z_R and Z_I are directly accessible from the impedance measurement. R_S, the solution resistance, has to be obtained from examining the complex plane impedance plot (c.f., Fig. 9). In the impedance plane plot, the imaginary value decreases with increasing frequency, until the curve approaches the real impedance axis. The real impedance is equal at this point to the solution resistance R_S. The value is independent of applied interfacial potential, but it depends on the position of the reference electrodes (different uncompensated resistance). Because the calculated capacitance is very sensitive to the calculated R_S, the placement of the reference electrodes must be carefully controlled.

Once R_S is determined, capacitance can be calculated from eq. 18 using only one set of impedances. The recommended approach is, however, to calculate C from all the frequencies obtained. This allows for averaging measurement uncertainty and it also allows to verify correctness of the calculation. In an ordinary system, the calculated capacitance should be independent of frequency. Any drift with frequency other than experimental noise indicates a possible problem. One cause for variation may be incorrect equivalent circuit used for the evaluation.

Evaluated interfacial capacitance is shown in Fig. 14 as a three–dimensional surface plot, charting the dependence of the capacitance on the BSA concentration and on the applied interfacial potential. The capacitance decreases with increasing concentration of the protein, until a plateau is reached.

Effect of pH on adsorbed BSA. The capacitance measurement is very useful in the study of protein adsorptive properties as a function of pH. Figure 15 shows the capacitance change as the pH was varied using the Robinson–Britton buffer. The capacitance is essentially invariant with the protein absent. Addition of the

protein has pronounced effect. The change of the charge of the adsorbed zwitterionic protein with the change of pH shows clearly the gradual ionization both in cationic and anionic state. As expected, at the isoelectric point, where all the lines intercept, only a small change of capacitance with protein concentration is observed. This behavior demonstrates positively the adsorption of ionized functional groups of the protein.

Impedance methods, applied in the described way, can be useful to understand films of biochemical materials adsorbed at liquid/liquid interfaces and can provide some information for modeling ion transport across a biological membrane.

MICROINTERFACE BETWEEN TWO IMMISCIBLE SOLUTIONS

The cell in Fig. 2 is a typical apparatus used in L/L studies. However, recently it has been shown, that small interfaces, called here microinterfaces, can be used with some experimental advantage. The purpose of this modification is to use the same advantage as the ultramicroelectrodes have. Ultramicroelectrodes help to overcome solution resistance difficulties originating from a potential shift arising from an uncompensated iR drop. As the interfacial area becomes smaller, the diffusion geometry becomes a spherically symmetric process. This means that the ratio of charge transport current versus solution resistance is increasing and, in the end, it renders the iR drop minimal. In ITIES studies, restricting the interfacial area and using a current amplifier for voltammetric studies is a viable alternative to a four–electrode potentiostat.

Small L/L interfaces have been used by Girault and co–workers (33–38) and by Senda et al. (39–40). We have used in our work a small hole formed in a

thin glass wall (41–43). Fig. 16 is a voltammetric response of lauryl sulfate anion transport between water and nitrobenzene. Recent analytical applications of these microinterfaces have resulted in construction of probes solidified by gels. The advantage of such a modification if ease of handling (44–47). The immobilization can be extended further to studies of frozen interfaces, or even to use solid electrolytes. Significantly, ITIES theory also applies to interfaces that are encountered in ion–doped, conductive, polymer–coated electrodes.

Fast scan voltammetry, in particular on microinterfaces, can be used for determination of charge–transfer rate constants. Impedance analysis can be used not only in analytical applications, but also to obtain a better understanding of surface phenomena (48) and adsorption (32). Microinterfaces, with their high own resistance, are well suited for impedance analysis derived from measurements of noise, generated by electrochemical system (49–50). Understanding the phenomena peculiar to microinterfaces is essential to the future studies of electrochemistry of small domains.

ACKNOWLEDGMENT

The research results described in this chapter and preparation of the manuscript has been supported by the Office of Naval Research.

Literature cited

1. Nernst, W. *Z. Phys. Chem.* **1888**, *2*, 613–637.
2. Blank, M.; Feig, S. *Science* **1963**, *141*, 1173–1174.
3. Koryta, J.; Vanýsek, P.; Březina, M. *J. Electroanal. Chem.*, **1976**, *67*, 263–266.
4. Vanýsek, P. *Anal. Chem.* **1990**, *62*, 827A–835A.
5. Vanýsek, P. *Electrochemistry on Liquid/Liquid Interfaces*; Springer: Berlin, 1985.
6. Koryta, J. In *The Interface Structure and Electrochemical Processes at the Boundary between Two Immiscible Liquids*; Kazarinov, V. E., Ed.; Springer: Berlin, 1987.
7. Girault, H. H. J.; Schiffrin, D. J. In *Electroanalytical Chemistry*; Bard, A. J., Ed.; Marcel Dekker: New York, 1989; Vol. 15.
8. Samec, Z. *Chem. Rev.* **1988**, *88*, 617–632.
9. Vanýsek, P; Buck, R. P. *J. Electrochem. Soc.* **1984**, *131*, 1792–1796.
10. Senda, M; Kakiuchi, T.; Osakai, T. *Electrochim. Acta* **1991**, *36*, 253–262.
11. Koryta, J. *Select. Electr. Rev.* **1991**, *13*, 133–158.
12. Waggoner, A. S. *Ann. Rev. Biophys. Bioeng.* **1979**, *8*, 47–68.
13. Bashford, C. L. *Biosci. Rep.* **1981**, *1*, 183–196.
14. Wiegand, D. H. Ph. D. Thesis, Northern Illinois University, DeKalb, 1990.
15. Hung, L. Q. *J. Electroanal. Chem.* **1980**, *115*, 159–174.
16. Parker, A. J. *Electrochim. Acta* **1976**, *21*, 671–679.
17. Rais, J. *Collect. Czech. Chem. Commun.* **1971**, *36*, 3253–3262.
18. Vanýsek, P. *Electroanalysis*, **1990**, *2*, 409–413.

19. Buck, R. P.; Vanýsek, P. *J. Electroanal. Chem.* **1990**, *292*, 73–91.

20. Vanýsek, P.; Buck, R. P. *J. Electroanal. Chem.* **1991**, *297*, 19–35.

21. Wiegand, D. H.; Vanýsek, P. *J. Colloid Interface Sci.* **1990**, *135*, 272–282.

22. Wiegand, D. H.; Vanýsek, P. *Appl. Spectrosc.* **1988**, *42*, 958–961.

23. Ehrenberg, B.; Montana, V.; Wei, M.–D.; Wuskell, J. P.; Loew, L. M. *Biophys. J.* **1988**, *53*, 785–794.

24. Gross, D.; Loew, L. M. *Fluorescent indicators of membrane potential: Microspectrofluorometry and imaging* In *Methods in Cell Biology*, Vol. 30, Ch. 7; Taylor, D. L.; Wang, Y.–L., Eds.; Academic Press, San Diego, 1989.

25. Åkerman, K. E. O.; Scott, I. G., Heikkilä, J. E., Heinonen, E. *J. Neurochem.* **1987**, *48*, 552–559.

26. Vanýsek, P. Ph.D. Thesis, Czechoslovak Academy of Sciences, J. Heyrovský Institute of Physical Chemistry and Electrochemistry, Prague, 1982.

27. Vanýsek, P.; Reid, J. D.; Craven M. A.; Buck, R. P. *J. Electrochem. Soc.* **1984**, *131*, 1788–1791.

28. Kakiuchi, T.; Yamane, M.; Osakai, T.; Senda, M. *Bull. Chem. Soc. Jpn.* **1987**, *60*, 4223–4228.

29. Yamane, M.; Kakiuchi, T.; Osakai T.; Senda, M. *Rev. Polarogr. (Kyoto)* **1983**, 2A26.

30. Wandlowski, T.; Račinský, S.; Mareček V.; Samec, Z. *J. Electroanal. Chem.* **1987**, *227*, 281–285.

31. Wandlowski, T.; Mareček V.; Samec, Z. *J. Electroanal. Chem.* **1988**, *242*, 277–290.

32. Vanýsek, P.; Sun, Z. *Bioelectrochem. Bioenerget.* **1990**, *23*, 177–194.

33. Taylor, G.; Girault, H. H. J. *J. Electroanal. Chem.*, **1986**, *208*, 179–183.

34. Campbell, J. A.; Stewart, A. A.; Girault, H. H. J. *J. Chem. Soc., Faraday Trans. I*, **1989**, *85*, 843–853.

35. Campbell, J. A.; Girault, H. H. *J. Electrcanal. Chem.* **1989**, *266*, 465–469.

36. Taylor, G.; Girault, H. H.; McAleer, J. *J. Electroanal. Chem.* **1990**, *293*, 19–44.

37. Stewart, A. A.; Shao, Y.; Pereira, C. M.; Girault, H. H. *J. Electroanal. Chem.* **1991**, *305*, 135–139.

38. Shao, Y.; Osborne, M. D.; Girault, H. H. *J. Electroanal. Chem.* **1991**, *318*, 101–109.

39. Senda, M.; Kakutani, T.; Osakai, T.; Ohkouchi, T. *Proceedings of the 1st Bioelectrochemical Symposium,* Mátrafüred, 1986, Akademiai Kiado, Budapest, pp. 353–364.

40. Ohkouchi, T.; Kakutani, T.; Osakai, T.; Senda, M. *Anal. Sci.* **1991**, *7*, 371–376.

41. Vanýsek, P.; Hernandez, I. C. *Anal. Lett.* **1990**, *23*, 771–785.

42. Vanýsek, P.; Hernandez, I. C.; Xu, J. *Microchem. J.* **1990**, *41*, 327–329.

43. Vanýsek, P.; Hernandez, I. C. *J. Electrochem. Soc.* **1990**, *137*, 2763–2768.

44. Kakutani, T.; Ohkouchi, T.; Osakai, T.; Kakiuchi, T. *Anal. Sci.* **1985**, *1*, 219–225.

45. Mareček, V.; Jänchenová H.; Colombini, M. P.; Papoff, P. *J. Electroanal. Chem.*, **1987**, *217*, 213–219.

46. Baum, G. *Anal. Lett.*, **1970**, *3*, 105–111.

47. Osakai, T.; Kakutani, T.; Senda, M. *Bunseki Kagaku,* **1984**, *33*, E371–E377.

48. Buck, R. P. *Ion–Select. Electr. Rev.* **1982**, *4*, 3–74.

49. Bezegh, A.; Janata, J. *Anal. Chem.* **1987**, *59*, 494A–508A.

50. Mareček, V.; Gratzl, M.; Pungor, A.; Janata, A. *J. Electroanal. Chem.* **1989**, *266*, 239–252.

51. Koryta, J.; Vanýsek, P.; Březina, M. *J. Electroanal. Chem.* **1977**, *75*, 211–228.

52. Vanýsek, P. *J. Electroanal. Chem.* **1981**, *121*, 149–152.

TABLE I

Standard potentials of transfer between water and nitrobenzene for ions used in the potentiometry measurements.

Ion	$\Delta_{\beta}^{\alpha}\varphi_i^o$ [mV]	Reference
Li^+	+ 395	51
Na^+	+ 354	51
H^+	+ 337	51
TMA^+	+ 35	51
TEA^+	− 59	51
TBA^+	− 248	51
$DiOC_1(3)^+$	− 310	21
$TPAs^+$	− 372	51
$DiOC_2(5)^+$	− 400	21
CV^+	− 410	52
Cl^-	− 324	51
I^-	− 195	51
TPB^-	+ 372	51

TABLE II

Slopes of the potential *vs.* logarithm of dye concentration plots at various dye concentrations and volume ratios of water to nitrobenzene.

Slope [mV/decade]

	dye concentration [mol l^{-1}]						
V_α/V_β	10^{-7}	10^{-6}	10^{-5}	10^{-4}	10^{-3}	10^{-2}	10^{-1}
10^5	0	0	0	− 2	− 6	− 70	− 70
10^4	0	0	− 0.5	− 3	− 29	−104	− 72
10^3	0	0	− 2	− 26	− 62	−106	− 70
10^2	0	− 2	− 26	− 57	− 62	−106	− 52
10	− 3.2	− 26	− 58	− 58	− 62	− 86	− 20
1	− 24	− 56	− 60	− 58	− 48	− 38	− 20
10^{-1}	− 50	− 56	− 50	− 38	− 32	− 34	− 22
10^{-2}	− 52	− 46	− 36	− 34	− 32	− 34	− 30
10^{-3}	− 40	− 34	− 32	− 32	− 38	− 46	− 36
10^{-4}	− 26	− 32	− 32	− 38	− 50	− 54	− 36
10^{-5}	− 12	− 27	− 38	− 50	− 58	− 54	− 36

Captions for figures:

Fig. 1 Comparison of (A) the interface between an electronically conductive electrode and a solution (reduction of Fe^{3+}) and (B) the interface between two immiscible solutions of electrolytes (ITIES) during current flow in a closed electric circuit (transport of picrate (Pi^-) from nonaqueous phase (n) to water (w)). (Reproduced from reference (4).)

Fig. 2 Apparatus used for potentiometric and voltammetric studies on the interface between two immiscible electrolyte solutions (ITIES). (Reproduced from reference (4).)

Fig. 3 Ion transport voltammogram of acetylcholine cation. 1 – Voltammogram of supporting electrolytes only: 1 mol l^{-1} LiCl in water and 0.025 mol l^{-1} tetrabutylammonium tetraphenylborate in nitrobenzene. 2 – after addition of 0.011 mol l^{-1} acetylcholine chloride to water. Scan rate 12.5 mV s^{-1}. (Reprinted from reference (9) by permission of the publisher, The Electrochemical Society, Inc.)

Fig. 4 Calculated interfacial potential as a function of the dye concentration for a system containing aqueous sodium chloride in concentrations ranging from 0 to 1 mol l^{-1} as indicated at the curves. 0.12 mol l^{-1} is a physiological saline solution (7 g l^{-1} NaCl). the dye $DiOC_1(3)I$ was dissolved in the nitrobenzene phase.

Fig. 5 Effect of the supporting electrolyte cation in the nitrobenzene phase on the relationship between interfacial potential and dye iodide ($DiOC_1(3)I$) concentration.

(A) 0.01 mol l^{-1} tetramethylammonium tetraphenylborate; (B)

0.01 mol l^{-1} tetraethylammonium tetraphenylborate; (C) 0.01 mol l^{-1} tetrabutylammonium tetraphenylborate; (D) two identical curves, one for 0.01 mol l^{-1} tetraphenylarsonium tetraphenylborate, and second for 0.01 mol l^{-1} crystal violet tetraphenylborate; without supporting electrolyte in nitrobenzene phase. Supporting electrolyte in water phase is always 0.01 mol l^{-1} LiCl, except (E), no supporting electrolytes.

Fig. 6 Calculated effect of supporting electrolyte concentration on potential – dye concentration relationship. The calculated interfacial potential is plotted *vs.* the logarithm of the ratio of the $DiOC_1(3)I$ dye concentration to the supporting electrolyte concentration.

Fig. 7 Relationship between interfacial potential and the logarithm of the initial $DiOC_1(3)$ concentration in the nitrobenzene phase. (A) Calculated potential of the working interface between 0.01 mol l^{-1} LiCl in water and 0.01 mol l^{-1} TBATPB in the presence of $DiOC_1(3)$, with the reference interface potential subtracted; (B) calculated potential of the reference interface between 0.01 mol l^{-1} TBACl in water and 0.01 mol l^{-1} TBATPB in nitrobenzene. Experimentally determined potential difference between the reference interface and the working interface for $DiOC_2(5)$ (o) and $DiOC_1(3)$ (□).

Fig. 8 Influence of an electroactive impurity on the interfacial potential – dye concentration relationship. The axis are x: logarithm of the dye concentration; y: logarithm of the ratio of water volume to nitrobenzene volume; z: difference between interfacial potential with and without the impurity. Standard potentials of transport for the

impurity cation $\Delta^{\alpha}_{\beta}\varphi^{o}_{+} = -100$ mV and for the anion $\Delta^{\alpha}_{\beta}\varphi^{o}_{-} = +100$ mV; c = $1x10^{-5}$ mol l^{-1}.

Fig. 9. Complex plane impedance plots of the water/nitrobenzene interface (negative imaginary impedance *vs.* real impedance) with and without bovine serum albumin. (•) supporting electrolyte only: 0.01 mol l^{-1} LiCl in water, 0.01 mol l^{-1} TBATPB in nitrobenzene. (o) addition of 3 ppm BSA in water. Applied interfacial potential 0.30 V (*vs.* TBA^{+} ion selective electrode), t = 25.0° C. Frequency of the measurement for selected values is indicated at the data points. (Reprinted with permission from reference (32).)

Fig. 10. Real (in phase) (top) and imaginary (out of phase) impedance as a function of applied interfacial potential at different BSA concentrations. Water: 0.01 mol l^{-1} LiCl, BSA concentration (ppm) (1) 0.0 (2) 0.5 (3) 3.0; Nitrobenzene: 0.01 mol l^{-1} TBATPB; f = 5 Hz, t = 25.0° C. (Reprinted with permission from reference (32).)

Fig. 11. Randles equivalent circuit used in the calculation of the interfacial capacitance. C – interfacial capacitance, R_S – bulk solution resistance, Z_W – Warburg impedance.

Fig. 12. Potential of zero charge of the water/nitrobenzene interface as a function of varying concentration of BSA in log(ppm). Supporting electrolytes 0.01 mol l^{-1} LiCl in water, 0.01 mol l^{-1} TBATPB in nitrobenzene.

Fig. 13. Real and imaginary impedance as a function of the concentration of BSA in aqueous phase at indicated frequencies. Water: 0.01 mol l^{-1} LiCl, nitrobenzene: 0.01 mol l^{-1} TBATPB. Applied interfacial

potential U = 0.35 V *vs.* TBA^+ ion selective electrode, t = 25° C. (Reprinted with permission from reference (32).)

Fig. 14. Three dimensional surface plot of the interfacial capacitance as a function of BSA concentration and applied interfacial potential. Water: 0.01 mol l^{-1} LiCl, nitrobenzene: 0.01 mol l^{-1} TBATPB, t = 25.0° C, Interfacial potential U given *vs.* TBA^+ ion selective electrode. (Reprinted with permission from reference (32).)

Fig. 15. The capacitance of the interface as a function of pH in the presence of different concentrations of BSA, buffered with Robinson-Britton solution. Water: 0.01 mol l^{-1} LiCl, BSA concentration (ppm): (1) 0.0, (2) 0.5, (3) 3.0, (4) 15.0; nitrobenzene: 0.01 mol l^{-1} TBATPB. Applied interfacial potential 0.30 V *vs.* TBA^+ ion selective electrode. (Reprinted with permission from reference (32).)

Fig. 16. Voltammetric determination of laurylsulfate (0.4 mmol l^{-1}) on a liquid/liquid microinterface. Scan rates (mV s^{-1}) (1) 10, (2) 20, (3) 50, (4) 100, (5) 200, (6) 500 and (7) 1000. Supporting electrolytes 0.02 mol l^{-1} LiCl in water and 0.02 mol l^{-1} TBATPB in nitrobenzene. Diameter of the hole 130 μm. (Reproduced from reference (4).)

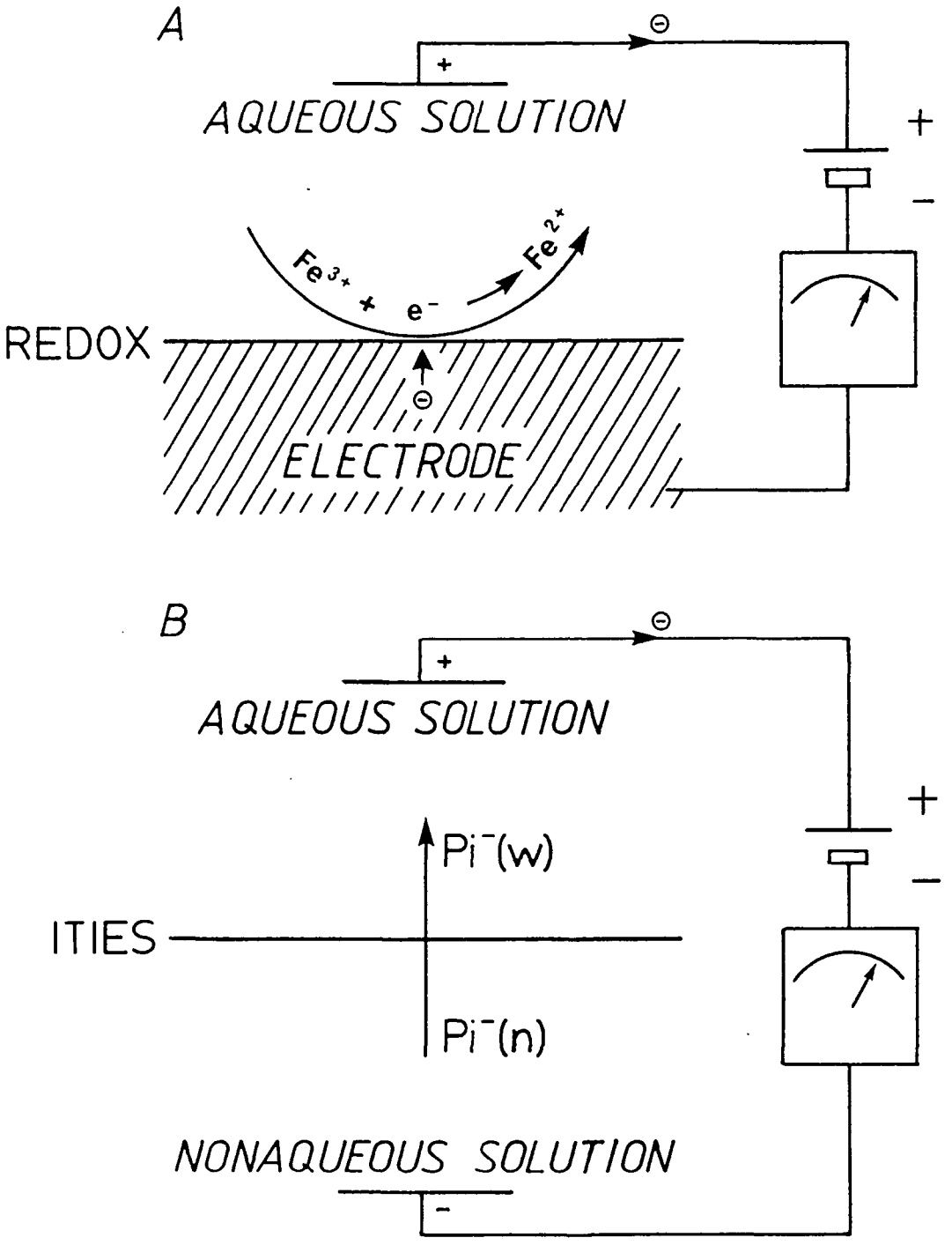

Vanýsek: Fig. 1

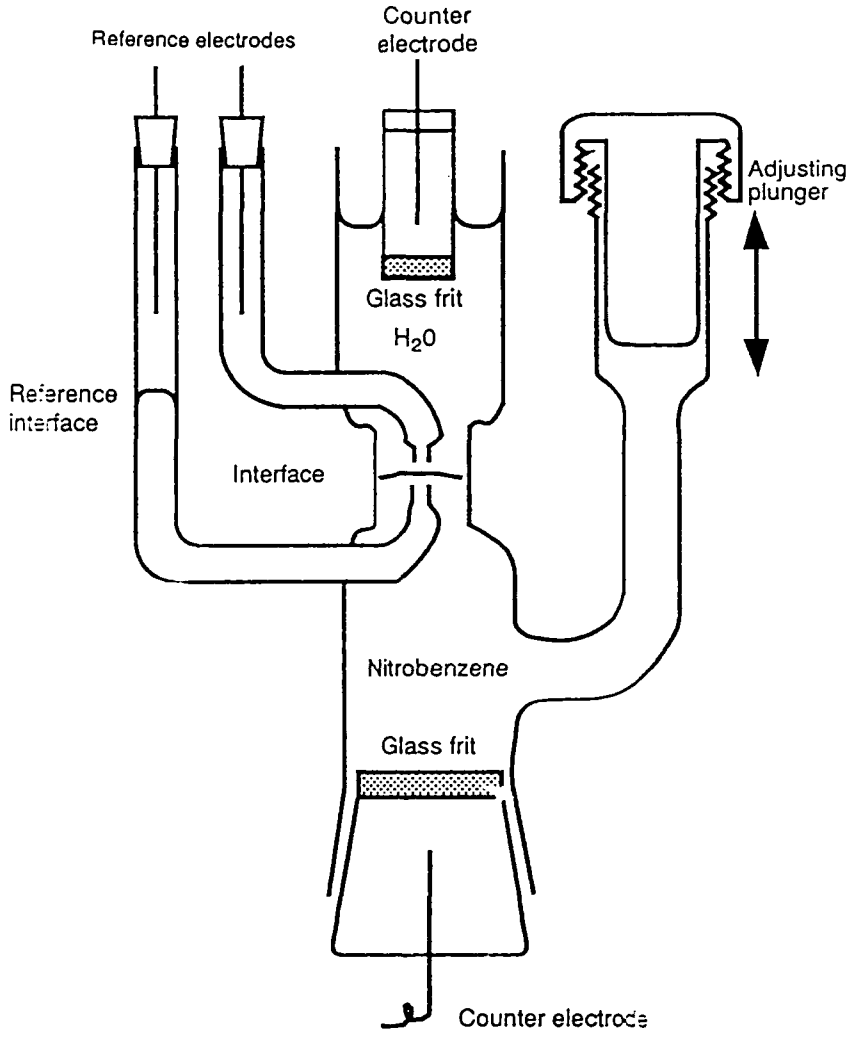

Vanýsek: Fig. 2

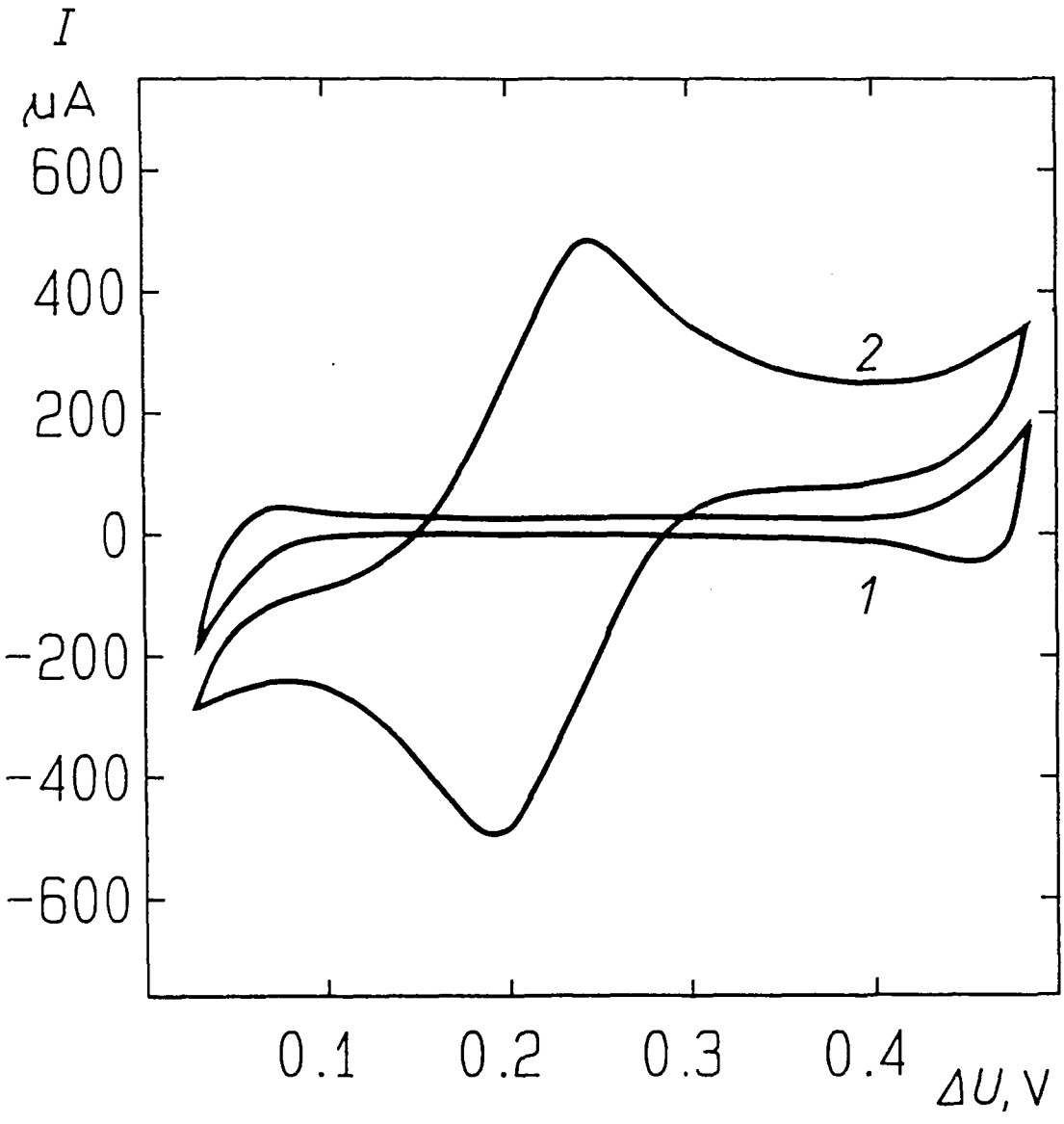

Vanýsek: Fig. 3

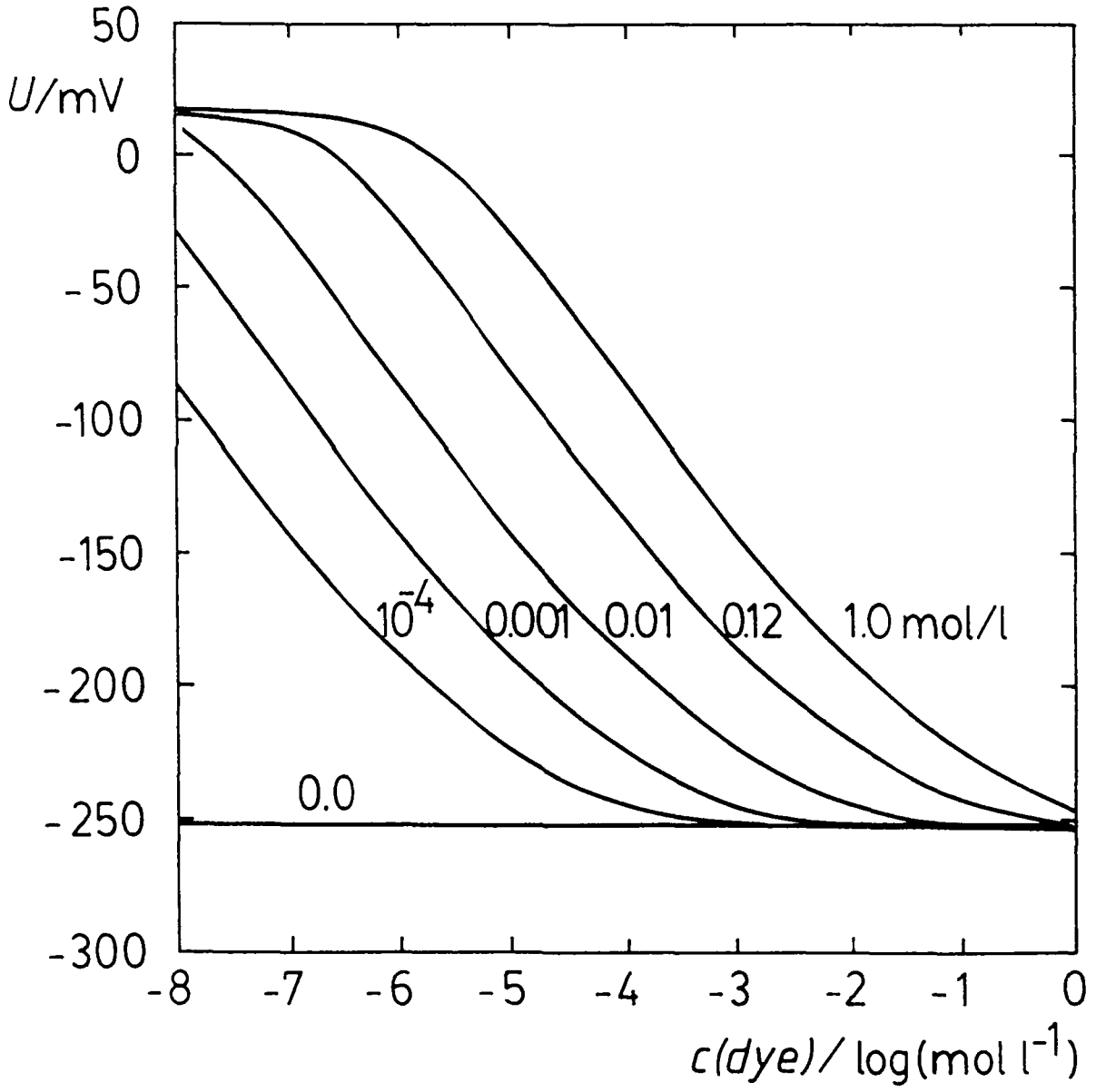

Vanýsek: Fig. 4

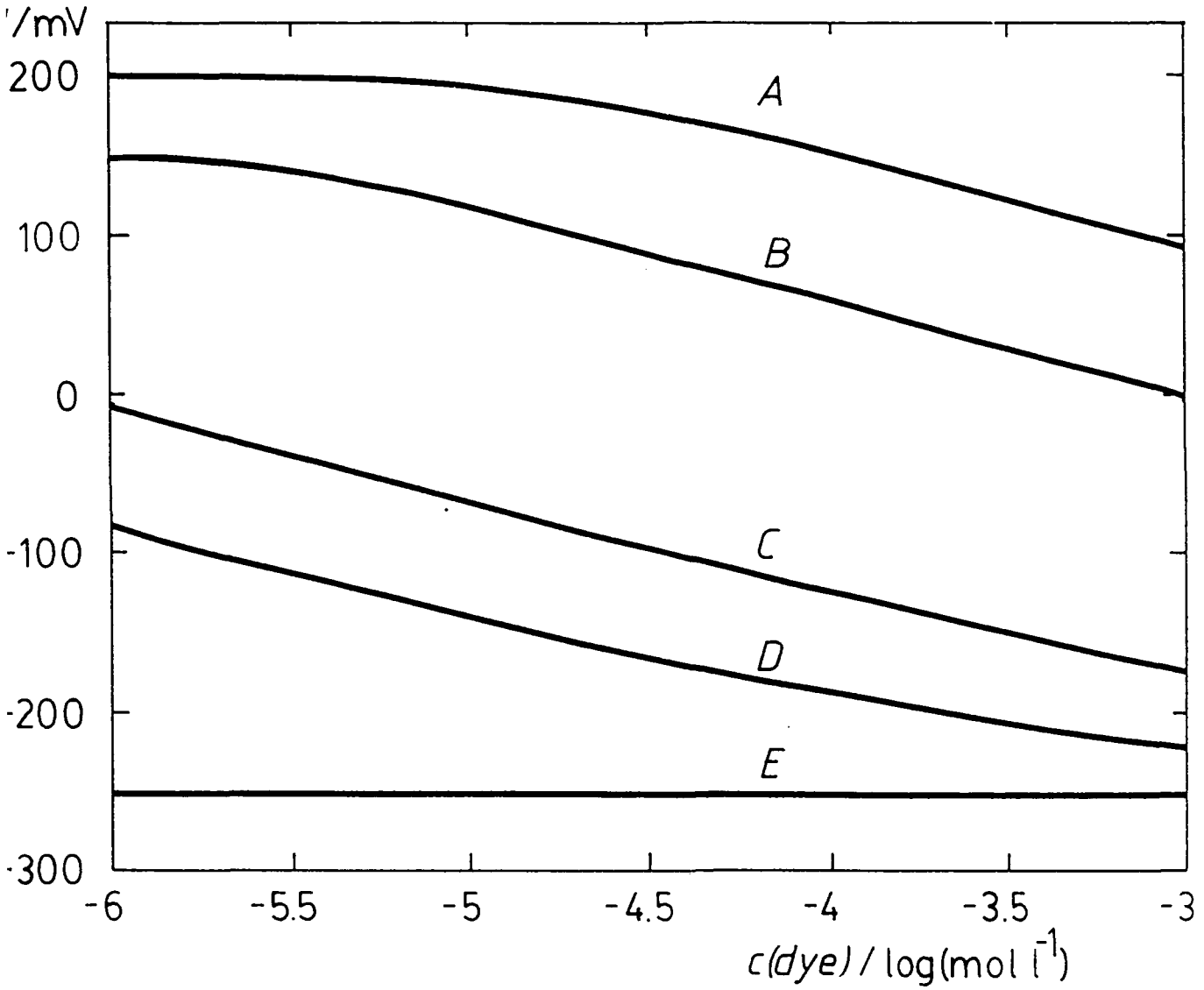

Vanýsek: Fig. 5

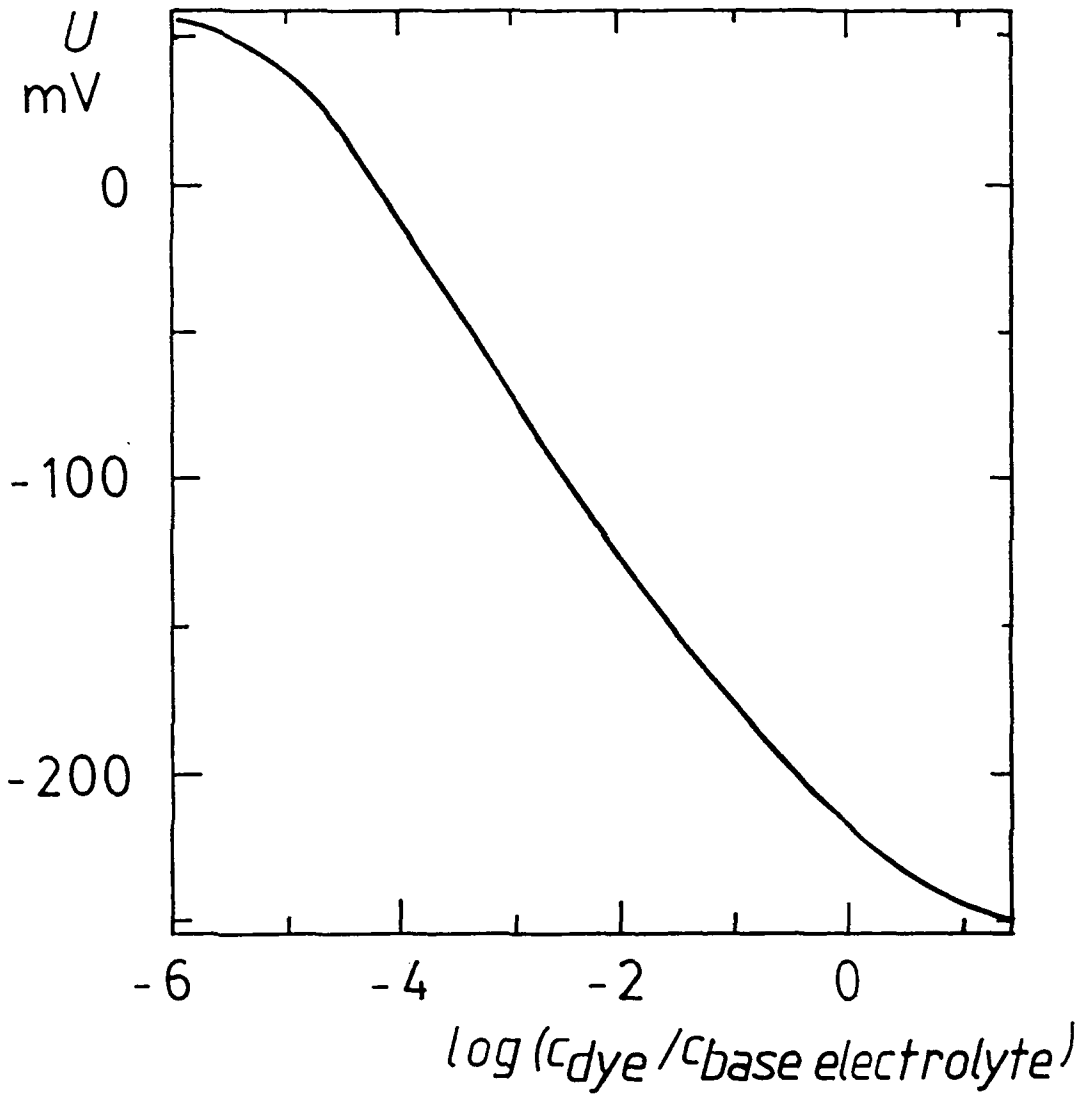

Vanýsek: Fig. 6

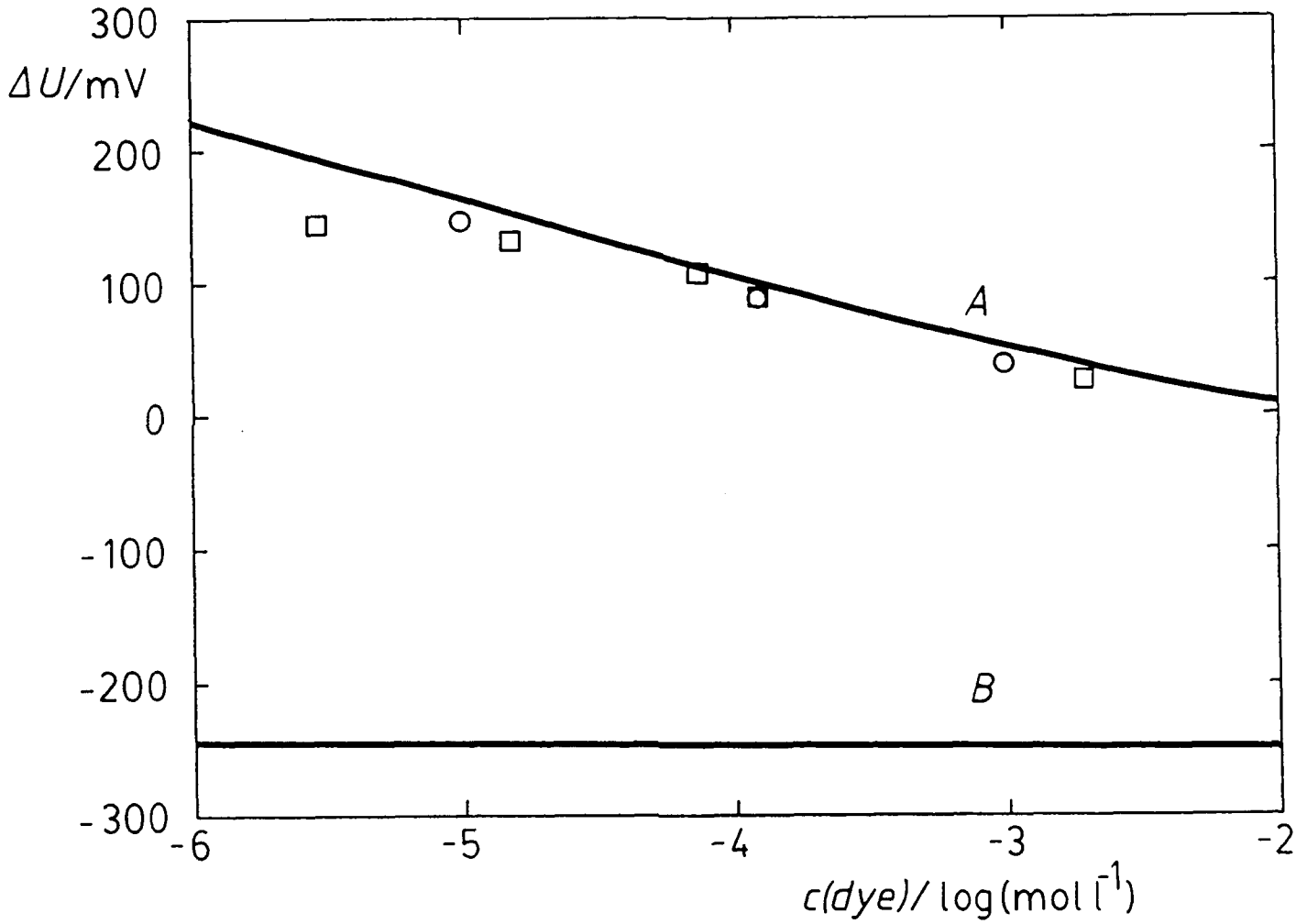

Vanýsek: Fig. 7

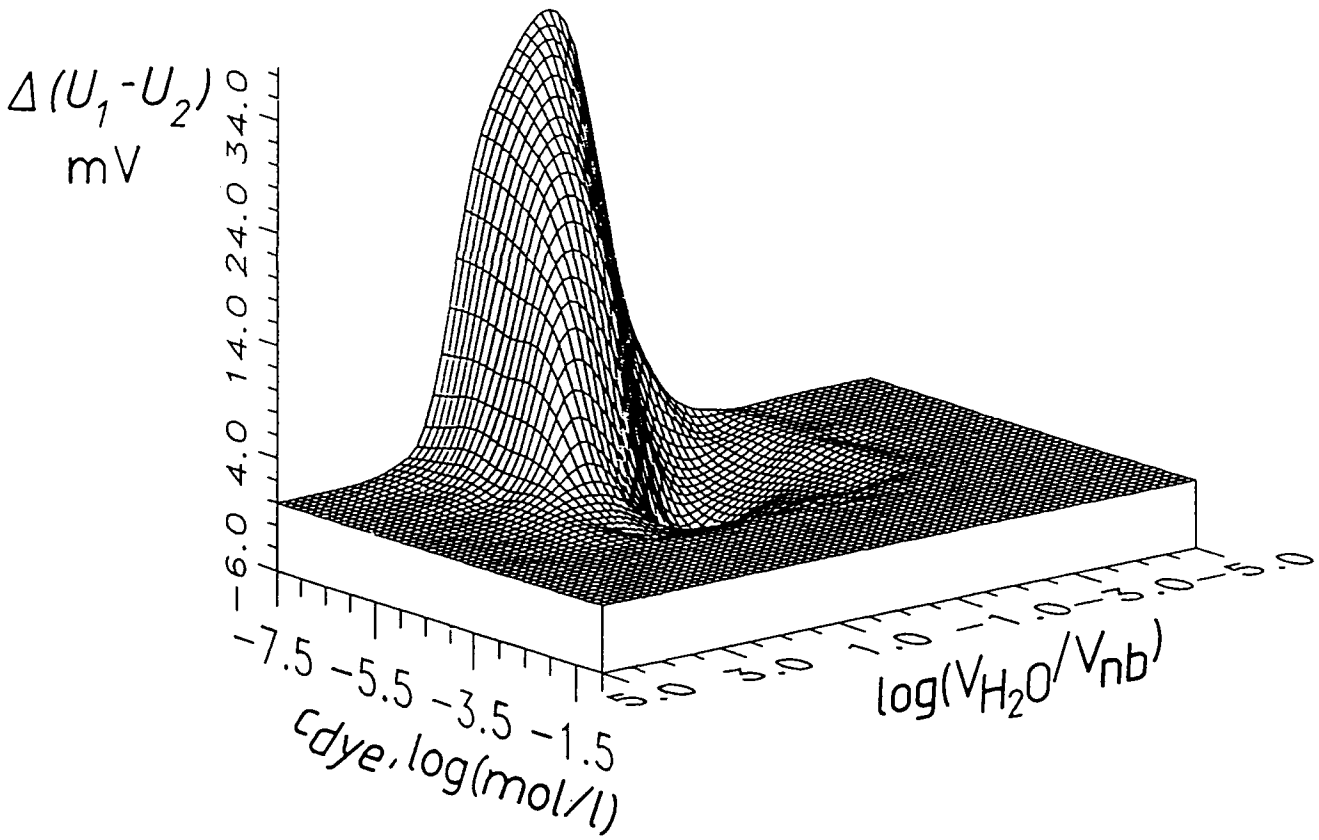

Vanýsek: Fig. 8

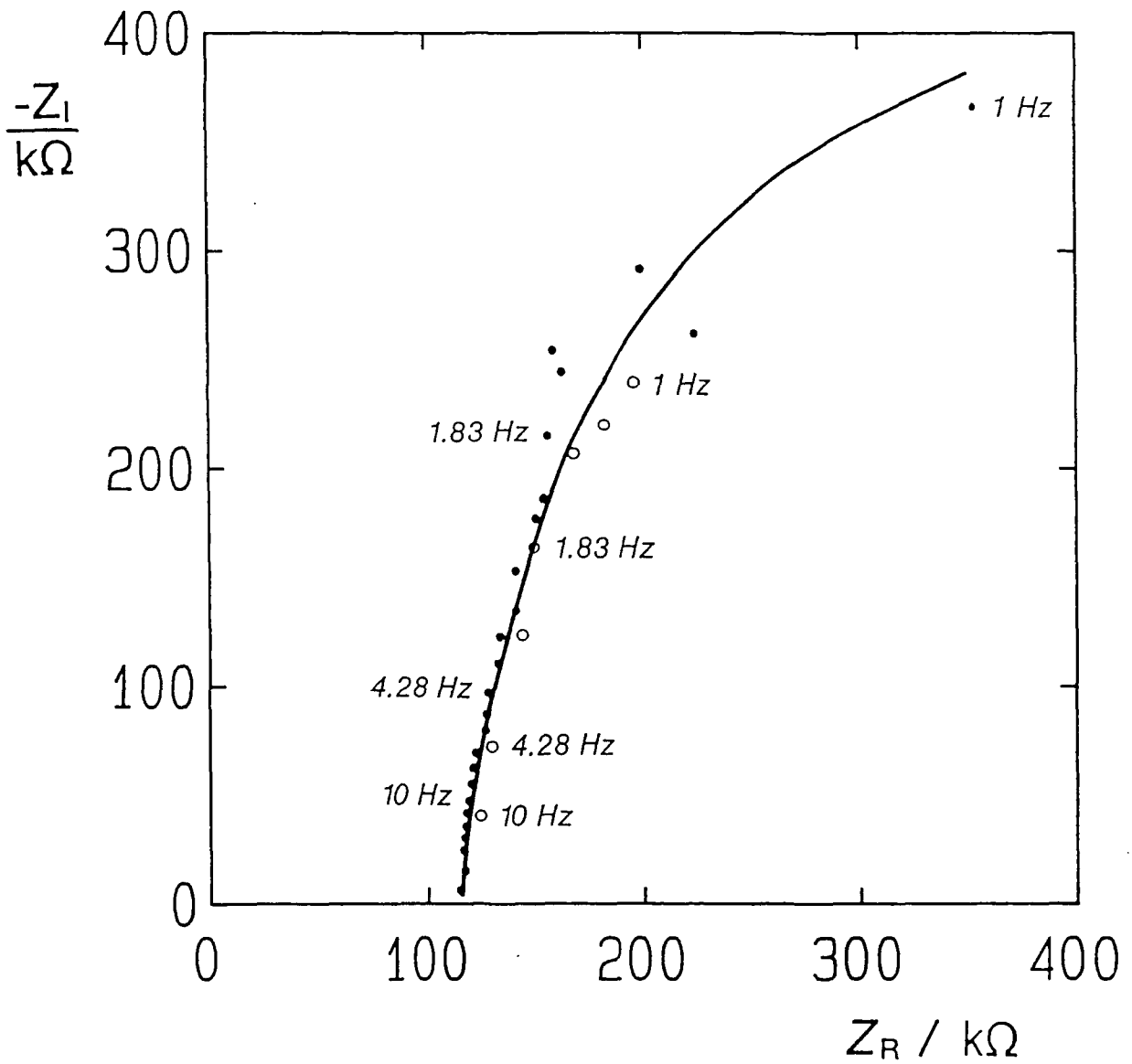

Vanýsek: Fig. 9

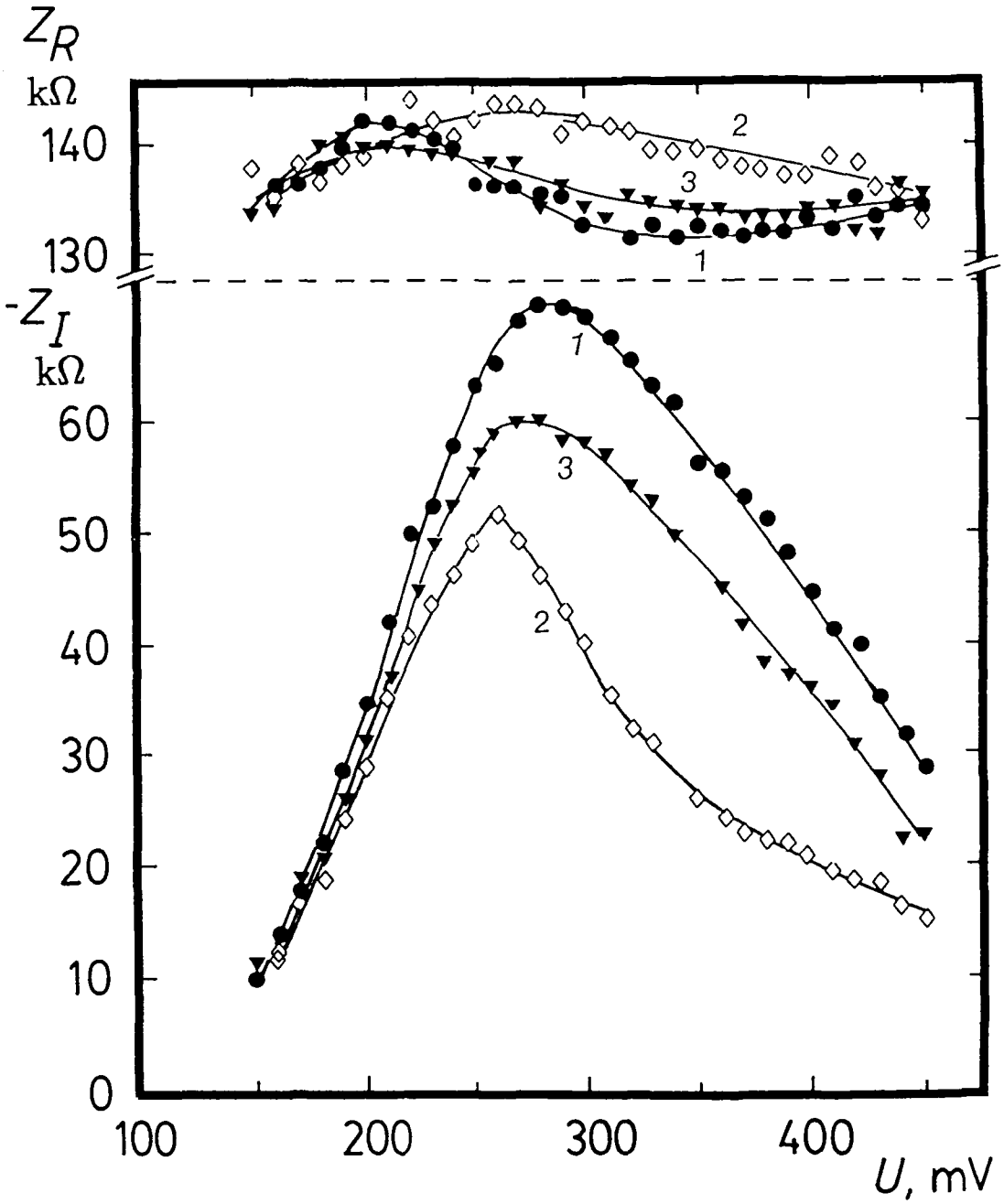

Vanýsek: Fig. 10

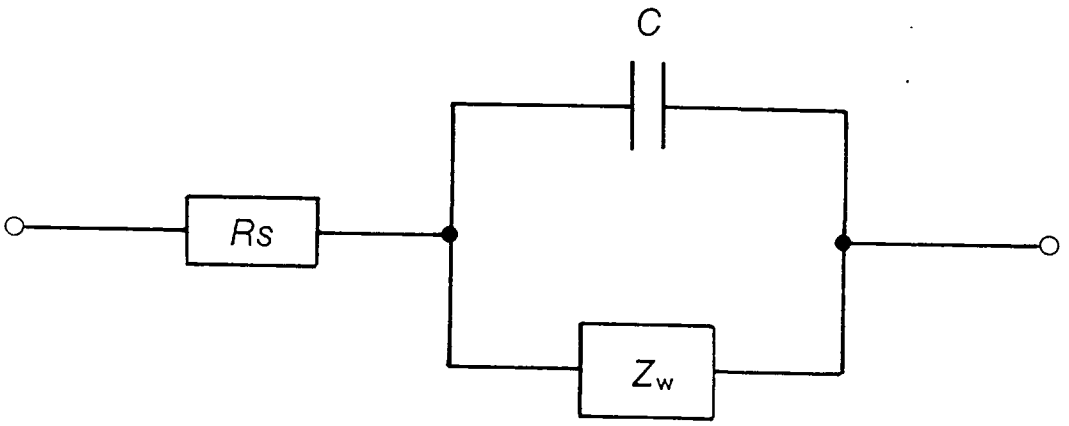

Vanýsek: Fig. 11

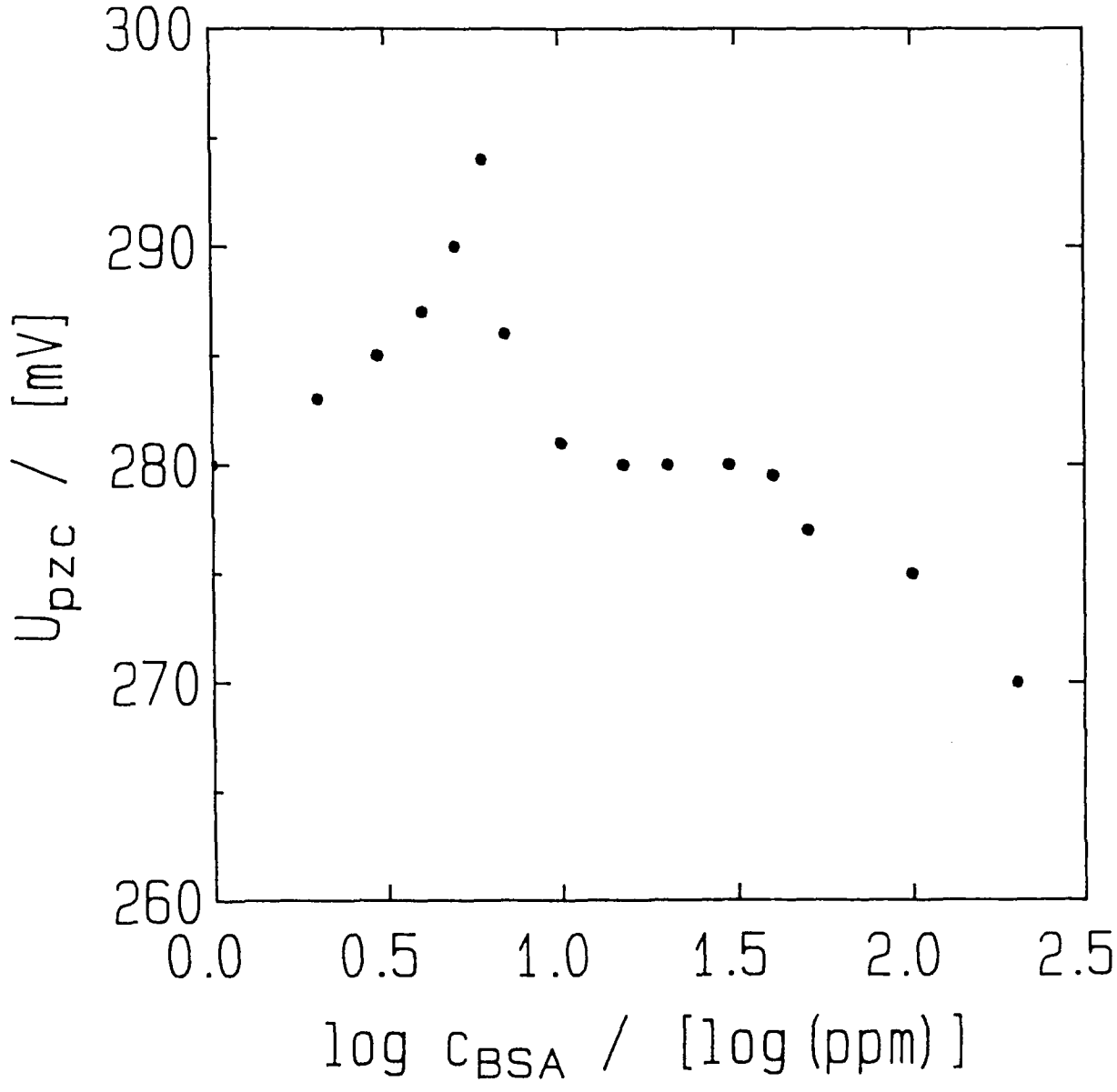

Vaňýsek: Fig. 12

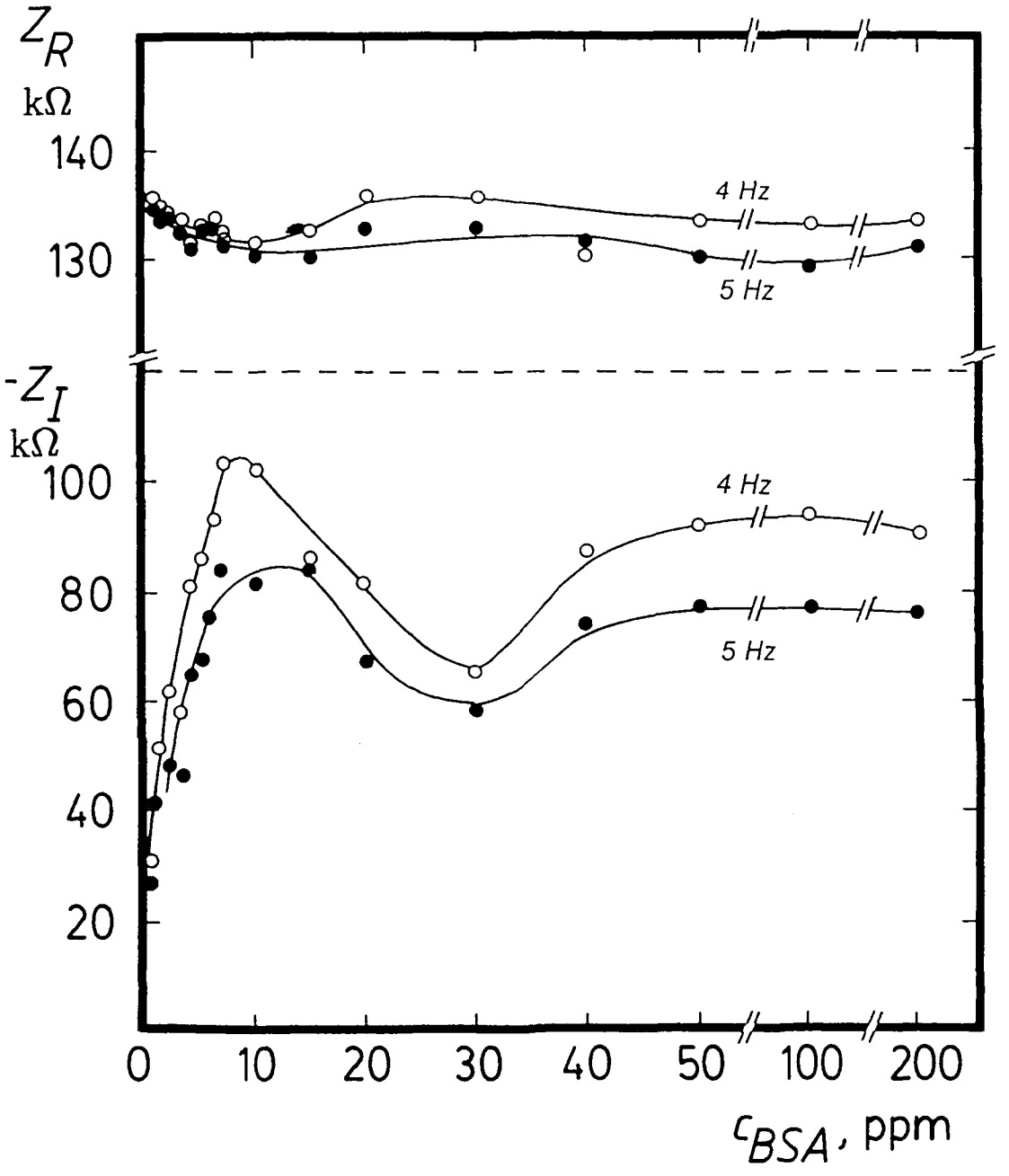

Vanýsek: Fig. 13

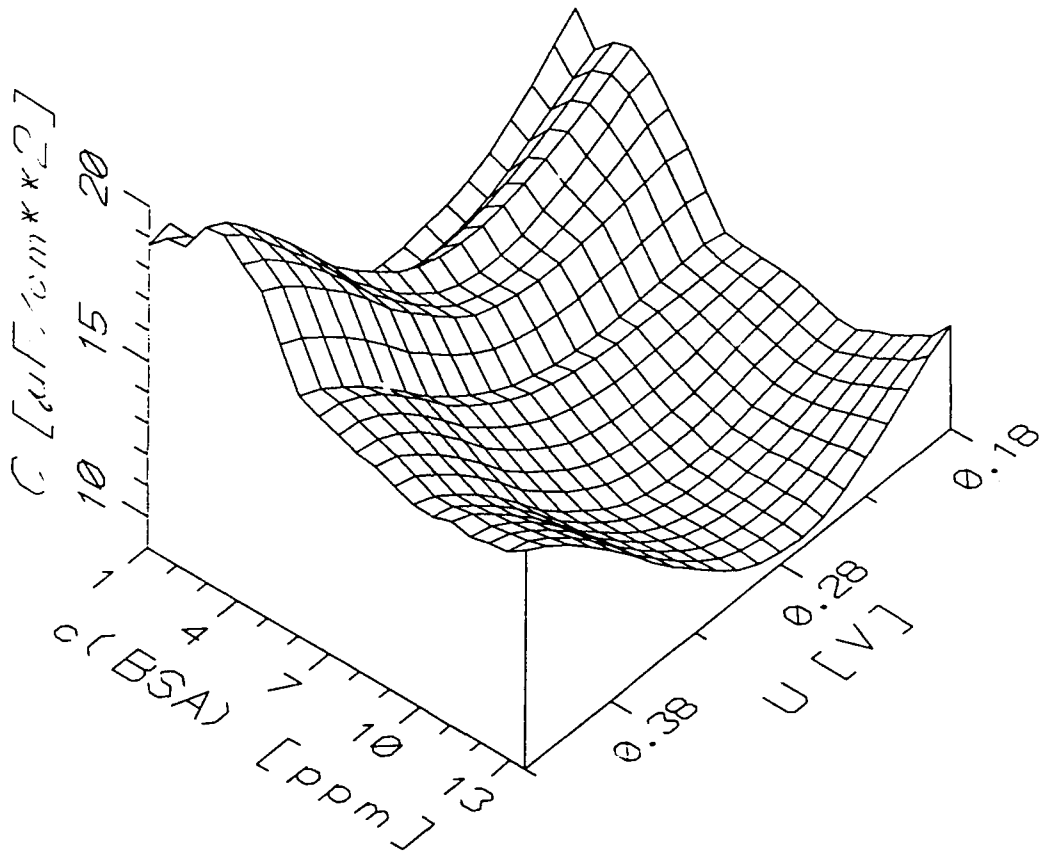

Vanýsek: Fig. 14

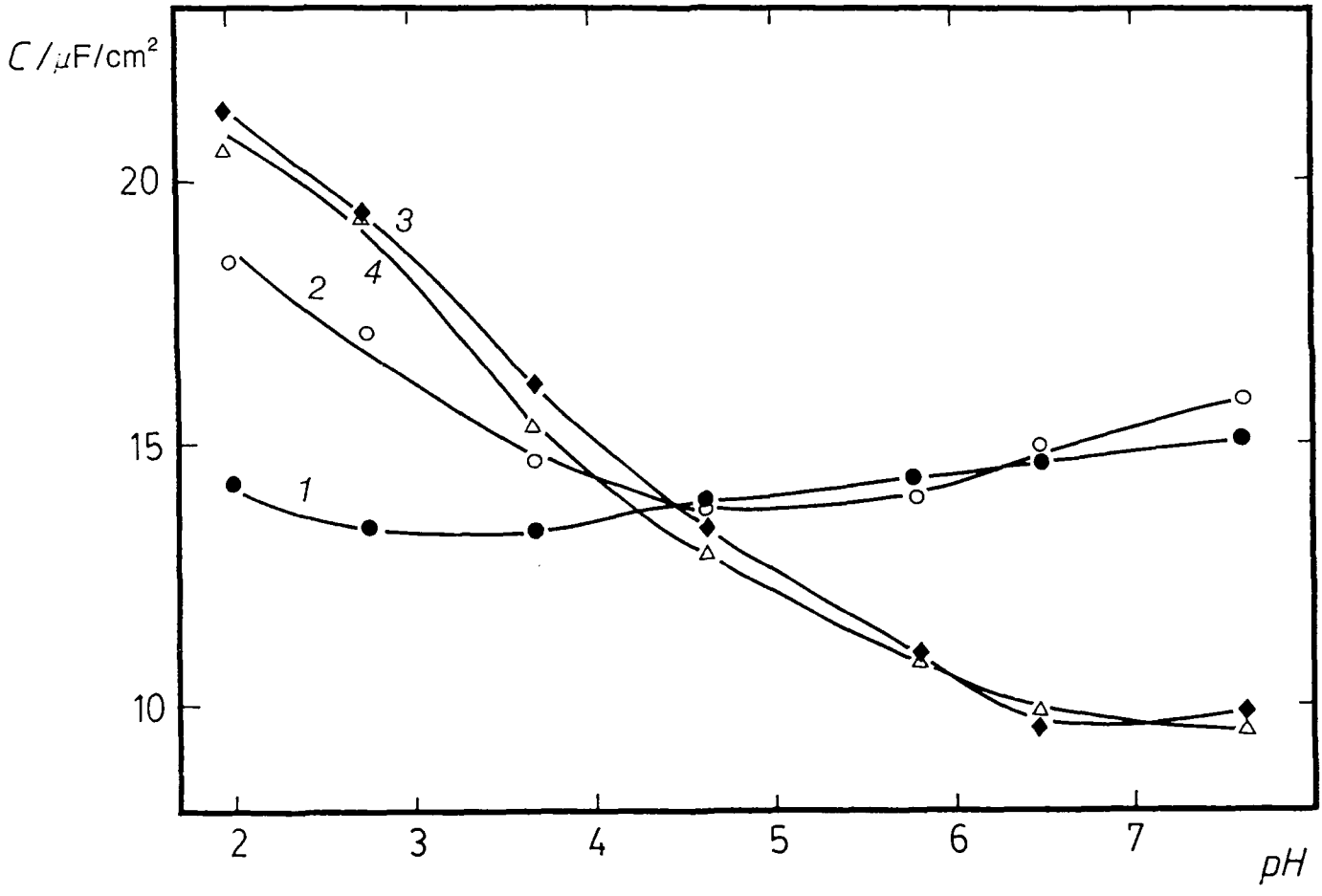

Vanýsek: Fig. 15

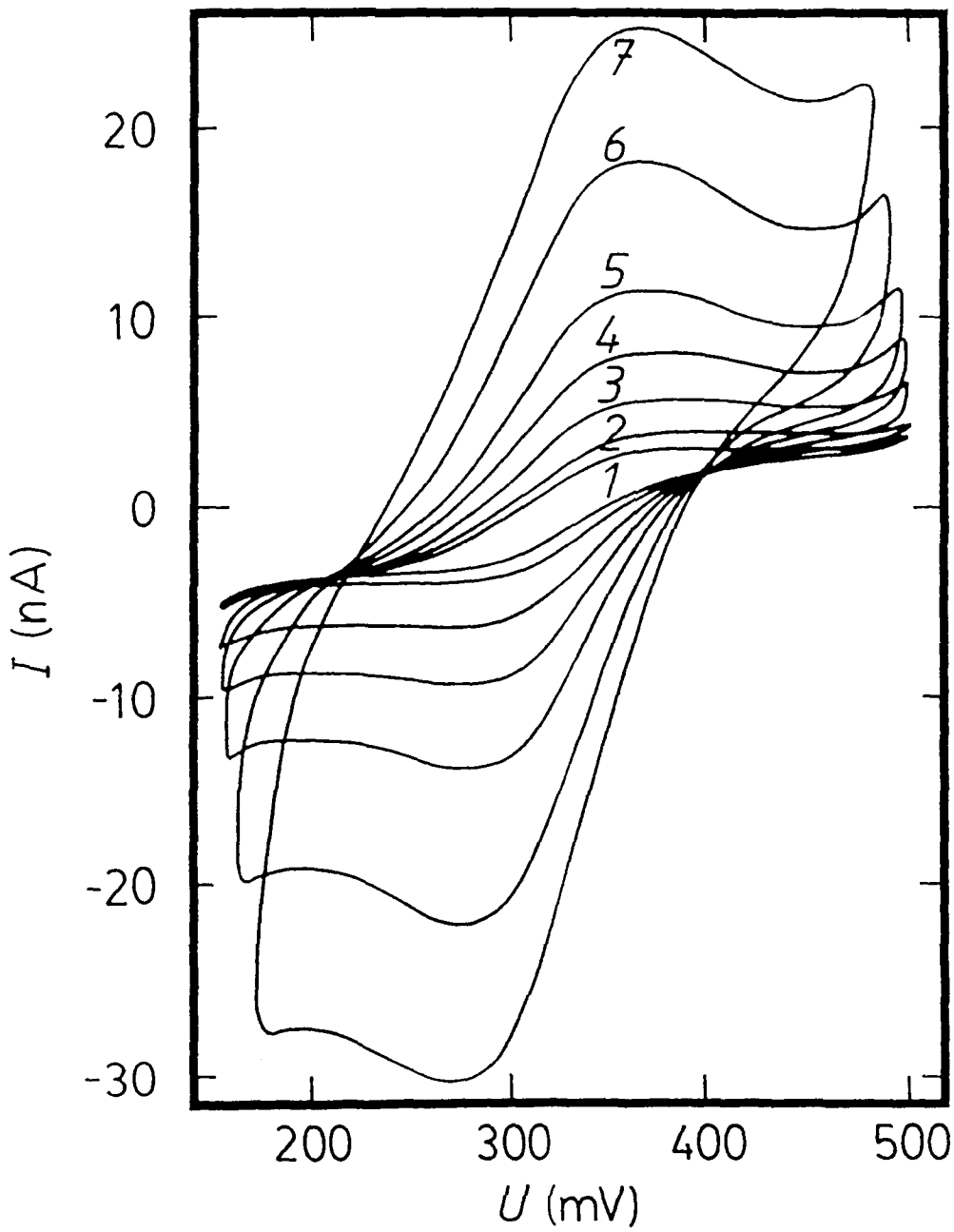

Vanýsek: Fig. 16

TECHNICAL REPORT DISTRIBUTION LIST - GENERAL

Office of Naval Research
Chemistry Division, Code 1113
800 North Quincy Street
Arlington, Virginia 22217-5000

Dr. James S. Murday
Chemistry Division, Code 6100
Naval Research Laboratory
Washington, DC 20375-5000

Dr. Robert Green, Director
Chemistry Division, Code 385
Naval Air Weapons Center
Weapons Division
China Lake, CA 93555-6001

Dr. Elek Lindner
Naval Command, Control and
Ocean Surveillance Center
RDT&E Division
San Diego, CA 92152-5000

Dr. Bernard E. Douda
Crane Division
Naval Surface Warfare Center
Crane, Indiana 47522-5000

Dr. Richard W. Drisko
Naval Civil Engineering
Laboratory
Code L52
Port Hueneme, CA 93043

Dr. Harold H. Singerman
Naval Surface Warfare Center
Carderock Division
Detachment
Annapolis, MD 21402-1198

Dr. Eugene C. Fischer
Code 2840
Naval Surface Warfare Center
Carderock Division
Detachment
Annapolis, MD 21402-1198

Defense Technical
Information Center
Building 5, Cameron Station
Alexandria, VA 22314